

1 **Joint Europa Mission (JEM)**

2 **A multi-scale study of Europa to Characterize its Habitability**

3 **and Search for extant life**

4 Michel Blanc⁽¹⁾, Nicolas André⁽¹⁾, Olga Prieto-Ballesteros⁽²⁾, Javier Gomez-Elvira⁽²⁾, Geraint Jones⁽³⁾,
5 Veerle Sterken^(4,5), William Desprats^(1,6), Leonid I. Gurvits^(7,16,38), Krishan Khurana⁽⁸⁾, Aljona Blöcker⁽⁹⁾,
6 Renaud Broquet⁽¹⁰⁾, Emma Bunce⁽¹¹⁾, Cyril Cavel⁽¹⁰⁾, Gaël Choblet⁽¹²⁾, Geoffrey Colins⁽¹³⁾, Marcello
7 Coradini⁽¹⁴⁾, John Cooper⁽¹⁵⁾, Dominic Dirkx⁽¹⁶⁾, Philippe Garnier⁽¹⁾, David Gaudin⁽⁶⁾, Paul Hartogh⁽¹⁷⁾,
8 Luciano Iess⁽¹⁸⁾, Adrian Jäggi⁽⁴⁾, Sascha Kempf⁽¹⁹⁾, Norbert Krupp⁽¹⁷⁾, Luisa Lara⁽²⁰⁾, Jérémie Lasue⁽¹⁾,
9 Valéry Lainey⁽²¹⁾, François Leblanc⁽²²⁾, Jean-Pierre Lebreton⁽²³⁾, Andrea Longobardo⁽²⁴⁾, Ralph Lorenz⁽²⁵⁾,
10 Philippe Martins⁽²⁶⁾, Zita Martins⁽²⁷⁾, Adam Masters⁽²⁸⁾, David Mimoun⁽⁶⁾, Ernesto Palumba⁽³³⁾, Pascal
11 Regnier⁽¹⁰⁾, Joachim Saur⁽²⁹⁾, Adriaan Schutte⁽³⁰⁾, Edward C. Sittler⁽¹⁵⁾, Tilman Spohn⁽³¹⁾, Katrin Stephan⁽³¹⁾,
12 Károly Szegő⁽³²⁾, Federico Tosi⁽³³⁾, Steve Vance⁽³⁴⁾, Roland Wagner⁽³¹⁾, Tim Van Hoolst⁽³⁵⁾, Martin
13 Volwerk⁽³⁶⁾, Frances Westall⁽³⁷⁾.

14 **Affiliations:** ⁽¹⁾IRAP, France ; ⁽²⁾INTA-CAB, Spain; ⁽³⁾MSSL/UCL, UK ; ⁽⁴⁾University of Bern,
15 Switzerland; ⁽⁵⁾ETH Zürich, Switzerland; ⁽⁶⁾ISAE, France; ⁽⁷⁾Joint Institute for VLBI ERIC, Dwingeloo,
16 The Netherlands; ⁽⁸⁾UCLA, USA ; ⁽⁹⁾Royal Institute of Technology KTH, Sweden, ⁽¹⁰⁾Airbus D&S, France,
17 ⁽¹¹⁾Univ. Leicester, UK; ⁽¹²⁾LPG, Univ. Nantes, France; ⁽¹³⁾Wheaton College, USA; ⁽¹⁴⁾CSEO, USA;
18 ⁽¹⁵⁾GSFC, USA; ⁽¹⁶⁾TU Delft, The Netherlands; ⁽¹⁷⁾MPS, Germany; ⁽¹⁸⁾Univ. Roma La Sapienza, Italy;
19 ⁽¹⁹⁾LASP, Univ. Colorado, USA; ⁽²⁰⁾IAA, Spain; ⁽²¹⁾IMCCE, France; ⁽²²⁾LATMOS, France; ⁽²³⁾LPC2E,
20 France; ⁽²⁴⁾IAPS, Italy; ⁽²⁵⁾APL/JHU, USA ; ⁽²⁶⁾Télécom ParisTech, France ; ⁽²⁷⁾CQE, IST, Portugal
21 ; ⁽²⁸⁾Imperial College, UK; CBM, France; ⁽²⁹⁾University of Cologne, Germany; ⁽³⁰⁾SKA Organisation, UK;
22 ⁽³¹⁾DLR, Germany; ⁽³²⁾WIGNER Institute, Hungary; ⁽³³⁾IAPS, Italy; ⁽³⁴⁾Jet Propulsion Laboratory, USA;
23 ⁽³⁵⁾ROB, Belgium; ⁽³⁶⁾IWF, Austria; ⁽³⁷⁾CBM-CNRS, France; ⁽³⁸⁾CSIRO Astronomy and Space Science,
24 Marsfield, NSW, Australia.
25

26 .

27

28

29

30

31 **ABSTRACT**

32 Europa is the closest and probably the most promising target to search for extant life in the Solar System,
33 based on complementary evidence that it may fulfil the key criteria for habitability: the Galileo discovery
34 of a sub-surface ocean; the many indications that the ice shell is active and may be partly permeable to
35 transfer of chemical species, biomolecules and elementary forms of life; the identification of candidate
36 thermal and chemical energy sources necessary to drive a metabolic activity near the ocean floor.

37 In this article we are proposing that ESA collaborates with NASA to design and fly jointly an ambitious
38 and exciting planetary mission, which we call the Joint Europa Mission (JEM), to reach two objectives:
39 perform a full characterization of Europa's habitability with the capabilities of a Europa orbiter, and
40 search for bio-signatures in the environment of Europa (surface, subsurface and exosphere) by the
41 combination of an orbiter and a lander. JEM can build on the advanced understanding of this system
42 which the missions preceding JEM will provide: Juno, JUICE and Europa Clipper, and on the Europa
43 lander concept currently designed by NASA (Maize, report to OPAG, 2019).

44 We propose the following **overarching goals** for our proposed Joint Europa Mission (JEM): **Understand**
45 **Europa as a complex system responding to Jupiter system forcing, characterise the habitability of**
46 **its potential biosphere, and search for life at its surface and in its sub-surface and exosphere.** We
47 address these goals by a combination of five Priority Scientific Objectives, each with focused
48 measurement objectives providing detailed constraints on the science payloads and on the platforms used
49 by the mission. The JEM observation strategy will combine three types of scientific measurement
50 sequences: measurements on a high-latitude, low-altitude European orbit; in-situ measurements to be
51 performed at the surface, using a soft lander; and measurements during the final descent to Europa's
52 surface.

53 The implementation of these three observation sequences will rest on the combination of two science
54 platforms: a soft lander to perform all scientific measurements at the surface and sub-surface at a selected
55 landing site, and an orbiter to perform the orbital survey and descent sequences. We describe a science
56 payload for the lander and orbiter that will meet our science objectives.

57 We propose an innovative distribution of roles for NASA and ESA; while NASA would provide an SLS
58 launcher, the lander stack and most of the mission operations, ESA would provide the carrier-orbiter-relay
59 platform and a stand-alone astrobiology module for the characterization of life at Europa's surface: the
60 Astrobiology Wet Laboratory (AWL). Following this approach, JEM will be a major exciting joint
61 venture to the outer Solar System of NASA and ESA, working together toward one of the most exciting
62 scientific endeavours of the 21st century: to search for life beyond our own planet.

63

64 Key words: outer planets exploration; search for life; Jupiter system; ocean moon; habitability.

65 **1. Scientific goals of JEM**

66 **1.1. Searching for extraterrestrial life in the Solar System.**

67 Astrobiologists agree today that the conditions for habitability are directly related to the definition of life
68 we can formulate on the basis of the only model of life we know, namely terrestrial life. From this
69 standpoint, habitable environments must meet three basic requirements symbolically represented by the
70 “Triangle of Habitability” (cf. Westall and Brack, 2018): 1) The presence of liquid water, which is the
71 best solvent known for inorganic and many small organic substances. The H₂O molecule has unique
72 properties that are specifically useful for life, e.g. latent heat due to the chemical bonds, potential for high
73 salt content due to its density, broad range of temperature and pressure stability, etc. 2) The availability of
74 life-essential chemical elements, such as H, N, C, O, S, P, as well as transition metals that help provide
75 structure to the biomolecules and provide nutrients to the organisms. Transition metals are made available
76 through the dissolution of the minerals. 3) Energy sources available for life to maintain metabolism. In the
77 absence of light, energy accessible for life is usually provided by chemical disequilibria sourced either by
78 radiation, reactions activated by temperature, or redox reactions. An additional key dimension to
79 planetary habitability is time. We do not know how quickly life appeared on Earth. The process must
80 have been sufficiently fast at the beginning to impede backward reaction, but the emergence of forms of
81 increasing complexity likely needed longer time scales, thus, implying the maintenance of habitability
82 conditions over very long times.

83 Based on these considerations, Lammer et al. (2009) explored the variety of known configurations of
84 planets and satellites to derive four classes of “habitable worlds”, or Habitats, as being the ones that meet
85 partly the habitability conditions. Classes I and II relate to our terrestrial planets (Earth, Mars, Venus),
86 and to the past or present existence of liquid water at their surface. Classes III and IV correspond to
87 objects where liquid water can be found, not at the surface, but in sub-surface oceans, which are found
88 among the icy satellites of Jupiter and Saturn: they are the “Ocean worlds”. Among them, Europa stands
89 out as one of the most promising destinations, and certainly the most promising one in the Jupiter System.
90 To understand why, let us first examine how the coupling of Europa to the Jupiter system may have
91 maintained it “inside the triangle of habitability”.

92 **1.2. Searching for life in the Jupiter system.**

93 *The Galilean satellites.*

94 In our search for life in the Jupiter System, the four Galilean satellites, sketched in figure 1, immediately
95 capture our attention. What we know of these moons today is essentially the legacy of the exploration of
96 the Jupiter System by the Galileo mission. First, we recognize three likely “ocean worlds”: Europa,
97 Ganymede and Callisto, whose sub-surface oceans, if confirmed, meet the first and most important
98 condition for habitability. If we then turn to their internal structure, the two innermost moons, Io and
99 Europa, are essentially “rocky moons”. Thus, Europa’s possible ocean must be in direct contact with the
100 thick silicate mantle which occupies most of its volume. A third important characteristics is that Io,
101 Europa and Ganymede are trapped in a 4:2:1 mean motion resonance, the so-called “Laplace resonance”,
102 which provides them with a continuous source of internal heating due to the dissipation of tidal motions.
103 Finally, both Io and Europa are recognized as “active moons”. While this is straightforward for volcanic
104 Io, the permanent resurfacing processes of Europa’s terrains places it as well in this category. Even more
105 importantly, a few repeated though still tentative observations by the Hubble Space Telescope (Roth et al.
106 2014) of plumes rising hundreds of kilometers above Europa’s surface indicate that Europa might be the
107 subject of geyser-like activity like Enceladus, though less intense. Evidence of plumes of water by these
108 marginal detections has been recently reinforced by two new observations, one from space and one from
109 the ground: first, a re-examination of in situ low European altitude magnetic field and plasma wave data
110 from Galileo, provided strong evidence that at least on one occasion this spacecraft flew through a dense
111 plume rising to at least 200 km above the surface (Jia et al., 2018); and secondly, direct searches for water
112 vapor on Europa spanning dates from February 2016 to May 2017 with the Keck Observatory resulted in
113 non-detections on 16 out of 17 dates, with upper limits below the water abundances inferred from
114 previous estimates. But on one date (26 April 2016) water vapor corresponding to a total amount of about
115 2000 tons was clearly detected on Europa’s leading hemisphere (Paganini, 2019). Taken together,
116 available observations support the idea that Europa plumes are real, though sporadic and perhaps rare
117 events.

118 Examined altogether, these four macroscopic properties point to Europa as the unique Galilean moon
119 likely bearing a subsurface ocean in direct contact with the silicate mantle (the very definition of a Class
120 III habitat), subject to tidal heating, and displaying signs of activity at its surface. Liquid water, a
121 permanent energy source, and access to heavy elements at the sea-floor: even a very superficial inspection
122 of the “triangle of habitability”, to be refined in detail later, provides a strong indication that Europa likely
123 stands “within the triangle”. For all these reasons we are now going to focus on a “systemic”
124 understanding of how this “Ocean world” is coupled to the Jupiter System, and on how the dynamics of
125 the coupled Europa/Jupiter-System may maintain habitability conditions at Europa.

126 ***Europa as a “Complex System” responding to Jupiter system forcing.***

127 One can describe Europa as a system of concentric and coupled layers, from the core to the exosphere and
128 the plasma envelope, responding globally to Jupiter system forcing. This forcing is essentially of two
129 types: gravitational (tidal) forcing, exerted mainly on the solid layers of Europa, and the electrodynamic
130 interaction of Jupiter’s corotating plasma, magnetic field and energetic particles with Europa’s
131 exosphere/ionosphere, surface and subsurface ocean.

132 **Tidal forcing.**

133 With a typical radius of 1500-2500 km, the four Galilean moons are large bodies inducing strong
134 gravitational perturbation to their environments throughout their orbital motions. Figure 2 illustrates the
135 Laplace resonance linking the mean motions of Io, Europa and Ganymede and shows the temporal
136 spectrum of the gravitational perturbations exerted on Europa (derived from Lainey et al., 2006). Because
137 of this orbital resonance, a dynamical equilibrium and continuous energy exchange are maintained
138 between the three innermost Galilean moons.

139 Tides are a major actor for heating the interior of the moons, with a heat flow up to 70 times the
140 radiogenic heating at Io (Hussmann et al. 2010). They affect both Jupiter and its moons. Because the
141 moons are synchronous, orbital eccentricity is the most evident way to allow for tidal forcing inside the
142 moons. Without the Laplace resonance, the eccentricity of the orbits would have been lost for long. But
143 the Laplace resonance forces the eccentricities of Io and Europa to substantial values while the orbits are
144 secularly evolving under tides.

145 In addition to the eccentricity of their orbits, the existence of an obliquity and large physical librations
146 may allow for tidal friction inside the moons too. For the Galilean system, the obliquities are believed to
147 be small, even though never measured so far (Bills & Ray 2000). The magnitude of physical librations
148 depends on the moment of inertia of the moons. The presence of an internal ocean may allow a
149 decoupling between the interior and the crust. Like for the obliquities, the physical librations of the
150 Galilean moons remain unmeasured. A clear measurement of the obliquities and physical librations will
151 allow a more accurate estimation of heating inside the bodies (Wisdom 2004).

152 On long time scales, the evolution of the Galilean system links the moons internal evolution with their
153 orbital one. While the moons are heating up (cooling down) their viscosity may decrease (increase),
154 allowing for significant feedback on the orbits. Studying such coupling, periodic solutions for Io’s heating
155 were pointed out by Ojakangas & Stevenson (1986) and Hussmann & Spohn (2004). More generally, the
156 origin of friction inside the moons remains to be discriminated. In icy bodies, significant tidal dissipation

157 may arise inside the silicate core, the ocean and the icy crust. While strong dissipation within the ocean
158 remains unlikely (Tyler 2008; Chen et al. 2014), tidal heating may play an important role within the
159 mantle (Moore (2003), Hussmann and Spohn (2004), Tobie et al. (2005)) and the icy crust (Cassen et al.
160 (1979), Tobie et al. (2005), Nimmo et al. (2002)).

161 This resonant coupling mechanism has important consequences for all moons. In the case of Europa, it
162 provides a permanent source of heating to the ice shell and mantle. But the temporal variation of total
163 tidal heating and its vertical distribution between mantle and ice shell are poorly constrained by
164 observations. Figure 3 shows a simulation result from Tobie et al. (2003) predicting that most of the tidal
165 heating goes into the ice shell, but this prediction has to be validated by adequate observations.

166 **Magnetospheric forcing.**

167 At the Jovicentric radial distance of Europa, the dynamics of the magnetosphere is dominated by three
168 phenomena: (a) Jupiter's field lines host the strongest radiation belts in the Solar System, whose harshest
169 region extends slightly beyond Europa's orbit ; (b) Jupiter's magnetic field lines corotate with the planet ;
170 (c) the dominant source of plasma is Io's volcanic activity, which results in the injection of about one
171 ton/s of fresh Iogenic ions into the corotating magnetic flux tubes. The centrifugal force acting on these
172 flux tubes drives an outward diffusion of this Iogenic plasma, which dominates all other plasma sources
173 throughout the inner and middle magnetosphere. At its radial distance, Europa is still imbedded inside the
174 Jovian radiation belts, and it opposes two types of obstacles to the Jovian corotating magnetic flux tubes
175 and plasma (Figure 4).

176 The first obstacle is the European surface. While the thermal plasma flow is deviated around this obstacle,
177 energetic particles bombard the surface, producing space weathering, particle absorption and desorption,
178 induced chemical reactions, and desorption of surface molecules. Some neutral exospheric particles
179 experience charge exchange with the incident magnetospheric flow. Charged particles freshly implanted
180 into the flow via pick-up are accelerated to tens of keV energies by Jupiter's strong corotation electric
181 field. In this way the European interaction adds ions of European origin coming from its exosphere or from
182 its surface, including ions of astrobiological interest, to the Jovian ion population.

183 In the sub-Alfvénic regime of this interaction, magnetic field lines first bend around this obstacle and pile
184 up, before being diverted around it. The velocity difference between this magnetized flow and the
185 European conductor induces a large potential drop, on the order of 200 kV, between the Jupiter-looking
186 side of Europa and the opposite side. This potential drop in turn drives a current system which flows
187 inside the tenuous ionosphere of Europa, before closing partly within the far-field Alfvén wings generated

188 by the obstacle, and partly through Jupiter's upper atmosphere. To understand the exchange of angular
189 momentum and of energy between Europa and the surrounding magnetospheric flow produced by this
190 interaction, one must be able to characterize the different components of this electrical circuit.

191 The second obstacle is the conducting ocean, which opposes the penetration of time-varying magnetic
192 field. The depth to which a signal is able to penetrate the conductor is given by the parameter:

$$193 \quad S = (\omega_{is}\mu\sigma_{is}/2)^{-1/2}$$

194 called the skin depth where ω_{is} is the frequency of the signal and σ_{is} the conductivity of the obstacle.
195 Galileo magnetometer data using Jupiter's rotating field as an 11-hour periodic signal unambiguously
196 confirmed the presence of a liquid water ocean but were not robust enough to place reliable constraints on
197 ice thickness, ocean thickness and ocean salinity. With its multiple flybys, the Europa Clipper mission
198 should be able to provide estimates of the inductive response of Europa's ocean at both the 11-hr and 85-
199 hour periods, and even of ocean thickness and conductivity within a certain domain of these parameters.
200 But a Europa Orbiter can provide estimates of signal strength and response over the much broader range
201 of frequencies of magnetic fluctuations experienced in the European environment (see fig. 4, insert) and
202 thus provide unique and accurate estimates of ice thickness, ocean thickness and ocean conductivity, as
203 will be shown in section 2.1.

204 ***Europa as a potential habitat***

205 In the context of a combined Europa orbiter-lander mission, we propose to re-examine now the
206 relationship of Europa to the "triangle of habitability" in the light of the coupling mechanisms of Europa
207 to the Jupiter system, which a Europa orbiter will be able to examine in unprecedented detail.

208 Based on the above reflections, there are several converging reasons for identifying the system formed by
209 the ice shell and internal ocean of Europa and their interfaces above (with the exosphere and Jovian
210 magnetosphere) and below (with the sea floor and silicate mantle), illustrated in Figure 5, as a potential
211 habitable world:

212 - Tidal interaction with Jupiter and the other Galilean satellites produces heat dissipation inside the
213 solid components of Europa, mantle and ice sheet, with a still unclear distribution between these
214 two sinks. This energy complements radiogenic heating and may play an important controlling role
215 in the maintenance of a liquid ocean, the activity of the rocky mantle and in the thickness of the ice
216 shell. The huge amount of energy available is manifested as geological features that deform the icy
217 crust around the globe. Some of them apparently are linked to aqueous reservoirs or the ocean. The

218 geological interpretation of these features indicates the possible presence of giant shallow lakes in
219 the subsurface, recent plume activity and diapirism, showing that the ice shell can mix vigorously:

220 - Europa's subsurface ocean is likely in direct contact with a silicate seafloor, possibly similar in
221 composition to the terrestrial ocean crust. It is an open question whether the rocky mantle is
222 geologically active, but if it is it may release essential elements for life: we know from terrestrial
223 analogues that catalytic reactions associated with hydrothermalism at the seafloor alter rocks,
224 making them porous, by favouring oxidation of minerals; they also produce oxidized and reduced
225 fluids, as well as organic compounds and hydrogen. Mg-sulfates that are observed on the icy
226 surface could be abundant in the ocean, forming from the oxidation of sulfides. Carbon species
227 such as carbonates, methane or other hydrocarbons can form from carbon dioxide or primordial
228 organics depending on the hydrogen fugacity or decomposition temperature.

229 - Apart from those produced during hydrothermal alteration of the rocks, other chemical gradients
230 are produced on the surface. The moon orbits well inside the Jovian radiation belts, whose particles
231 have direct access to its surface where they induce a host of radiolytic processes on the surface
232 material, including the synthesis of oxidizers, again a source of free energy. Europa thus has the
233 potential of displaying a redox couple between its sea floor and its surface, which can be a source
234 of chemical energy if the oxidized species can be transported through the ice shell by endogenous
235 processes, such as subduction as proposed by Kattenhorn and Prockter (2014). Galileo/NIMS first
236 detected distortions in the water ice absorption bands occurring between 1 and 3 μm reveal the
237 existence of non-ice material mixed with water ice at specific locations on the surface of Europa.
238 They have been identified as hydrated salt minerals like Mg-, Na-, Ca- sulphates, chlorides,
239 perchlorates and carbonates (endogenous), hydrated sulphuric acid and hydrogen peroxide
240 ($\text{H}_2\text{O}_2 \cdot 2\text{H}_2\text{O}$) (exogenous), or a combination of these three classes of compounds in varying
241 proportions across the surface (McCord et al., 1999; Dalton et al., 2005; Dalton et al., 2010;
242 Carlson et al., 2005; Loeffler and Baragiola, 2005; Brown and Hand 2013; Hanley et al., 2014).
243 Many of these chemical elements may be related to catalysis of prebiotic molecules. In particular,
244 magnesium may play a major role in stabilizing prebiotic molecules and catalysing more complex
245 molecules (Russell et al. 2014). On the other hand, other compounds would also have an exogenous
246 origin, such as silicates from impact materials (Zahnle et al. 2008) and sulphur species from Io and
247 elsewhere that take part in a radiolytic S cycle on the surface (Carlson et al., 1999).

248 Provided that the ice shell is "partly permeable" to the transfer of chemical species between the
249 liquid ocean and the icy surface, two key cycling processes may co-exist there:

250 - a net transport of radiolytically produced oxidizing species from surface to the liquid mass of the
251 ocean;

252 - conversely, the possibility of transfer of biomolecules and even of specific forms of life from the
253 deep ocean to the surface (more likely, to the sub-surface because of the radiation conditions there),
254 or even to erupting plumes, as will be discussed later.

255 Under these assumptions, the sub-system of Europa extending from the ocean silicate floor to the ice shell
256 surface, which corresponds exactly to the region of overlap between the domains of influence of tidal and
257 magnetospheric forcing, constitutes a candidate “European biosphere” worth characterizing by means of
258 quantitative measurements.

259 **The potential dark biosphere of Europa.**

260 How could life possibly emerge in this putative European biosphere? Of all existing scenarios, abiogenesis
261 at hydrothermal vents, with their highly reactive surfaces and protective porous niches, is favored by
262 many (e.g. Baross and Hofmann 1985; Russell and Hall, 1997). In terrestrial hydrothermal vents, the
263 building blocks of life were concentrated in the pores of the rocks, stabilized and assembled with the aid
264 of mineral surfaces. The process had to be kinetically fast and in one direction with estimates of the time
265 necessary ranging from some tens/hundreds of thousands to a few million years (Westall and Brack,
266 2018). The living cells that emerged from this process were very simple, even compared to the simplest of
267 living cells today. They consisted of hydrophilic molecules (long chain lipids) forming membranes that
268 separated the molecules (proteins) undertaking the process of living reactions (metabolism), i.e. obtaining
269 nutrients from the external environment and transforming them into energy and other molecular
270 components of cells, as well as molecules capable of encoding and transmitting information (e.g. RNA,
271 DNA and their as yet unknown predecessors). These first cells were fuelled on Earth by ingredients
272 provided by simple organic molecules, as well as hydrogen, produced by Fischer-Tropsch alteration of the
273 hot crust by circulating seawater and hydrothermal fluids, or released from organic rich fluid inclusions in
274 ultramafic rocks. Their carbon source was either inorganic CO₂ dissolved in the seawater (degassed by
275 differentiation and dissolved from the early CO₂ atmospheres), or the simple organic molecules provided
276 by hydrothermal activity or dissolved from the relatively abundant organic matter raining down on the
277 various bodies in the early Solar System in the form of carbonaceous meteorites, and comets. Such
278 chemotrophic cells would have formed colonies, possibly even biofilms on the surfaces of rocks and
279 minerals bathed in the hydrothermal fluids. Their abundance and distribution would have been strictly
280 controlled by access to nutrients, as was the case on the early Earth.

281 If there is continued hydrothermal activity on the seafloor of Europa, the most likely forms of life to have
282 lived possibly in the past and at present would be chemotrophs. These are surface specific life forms
283 whose biomass development and distribution is controlled by access to hydrothermal fluids and chemical
284 gradients. For possible traces of life on Europa to be detected today, either extant or extinct, it will be
285 necessary for the traces to be transported up to the base of the ice shell and through it towards the surface.
286 Under this restricting assumption, how can we design a “winning strategy” for our quest for life there?

287 **1.3. Searching for life at Europa.**

288 An efficient strategy to search for life at Europa must encompass three main types of contexts: the
289 biological, the chemical, and the geological/geophysical contexts. Traces of extant or extinct life could be
290 found potentially at the surface and near-surface environment of the ice, incorporated through reworking
291 (impact gardening, mass wasting and internal dynamics) of material brought up from aqueous reservoirs,
292 or in plumes of oceanic water spewed up into the exosphere: those are the places to look for. But bio-
293 signatures, if they exist, will be strongly influenced by the extreme environmental conditions reigning on
294 the surface of the ice and in the exosphere – high radiation, production of corrosive oxidizing species and
295 radicals, tenuous atmosphere and low water activity. This would lead to rapid death of living cells and
296 rapid degradation of the organic components of life. The remnant organic molecules are likely to be
297 refractory, particularly if they have been exposed to the surface for long periods of time. Therefore, the
298 search for signs of life needs access to fresh endogenic materials, which should be coming from the
299 habitable environment in the case of extant life, and must be performed with a specific instrumentation
300 and in the appropriate layers:

301 - Subsurface sampling, a must in our strategy, must search for better protected samples that could be
302 analysed in different physical states (solid/liquid). Analysis of samples in the aqueous phase will be
303 obtained by melting near-surface ice samples, while chemical disequilibria will be simultaneously
304 characterized during the search for biosignatures. The choice of performing our biomolecule
305 characterization measurements in liquid rather than in solid phase depends on the type of biosignature and
306 on the analytical procedure of identification, as will be explained in section 2.3.

307 - Capturing compounds in a plume, if and when it occurs, is another indirect way to access to material
308 emerging from the sub-surface. Evidences of water plumes erupting from the surface up to 200 km
309 around the southern hemisphere have been reported by Hubble Space Telescope images (Roth et al. 2014,
310 NASA report 26/09/2016). Ejecting materials would be coming from the interior of Europa, potentially
311 from liquid layers, so they could include important information about the habitable environments or even
312 evidences of life, as will be discussed further in section 2.2 and 2.3. This discovery offers a unique

313 opportunity to access the interior materials. Details of how this phenomenon occurs in Europa are still
314 unknown. Several mechanisms of plume production have been proposed for Enceladus, and the same
315 might work on Europa (Porco et al., 2006; Kiefer et al., 2006; Schmidt et al., 2008). Not all of them involve
316 liquid water: some of them are based on pressure changes in ice layers. The example of Enceladus shows
317 that an oceanic origin can be considered if salt or other specific mineral grains are detected by future
318 observations.

319

320 **1.4. JEM: the next logical step in NASA and ESA strategies for Jupiter System exploration.**

321 The design and planning of JEM will be able to rest on the unique asset of several missions to the Jupiter
322 System to be flown by ESA and NASA in the coming decade: Juno (NASA), JUICE (ESA) and most
323 importantly Europa Clipper. The host of data on Europa this mission will return from its 45 fly-bys will
324 provide the necessary basis for the design of a lander mission, which is already under study by NASA.
325 The overarching goal of JEM, complementary to its predecessors at Jupiter, can be formulated as follows:

326 **Understand Europa as a complex system responding to Jupiter system forcing, characterize the**
327 **habitability of its potential biosphere and search for life at its surface and in its sub-surface and**
328 **exosphere.**

329 To address this goal, the science plan of JEM, schematically represented in figure 6, will study Europa as
330 a system of coupled layers at three scales: the global scale (European radius), a medium scale (the
331 thickness of Europa's potential biosphere), on the basis of five priority science objectives.

332 **2. Detailed scientific objectives and measurement requirements.**

333 For each of our five science objectives, we describe now the corresponding measurement requirements
334 and constraints on the mission profile, which are summarized in the Science Traceability Matrix of JEM
335 (Annex I).

336 2.1. Global scale science investigations: Understand Europa as a system of coupled layers
337 responding to Jupiter System forcing.

338 **PSO#1: Determine the global structure of the European magnetic field and plasma environment**
339 **including potential plume characterization, and the associated response of Europa, including its**
340 **ocean, to Jupiter System magnetospheric forcing.**

341 The interaction of Europa with the Jovian magnetospheric field and flow results in the complex
342 distribution of plasmas, energetic particles, magnetic fields and electric currents illustrated in Figure 4.
343 The resulting charged particle population is a complex mixture of ions of different origins: to the primary
344 population of Iogenic ions, dominant in the Jovian plasma sheet, the European interaction adds ions of
345 European origin coming from its exosphere, or even directly from its surface, or from its subsurface
346 through potential plumes, into the magnetospheric flow. Measuring its chemical composition bears a high
347 astrobiological potential, since biomolecules present in Europa's surface layer may have made their way
348 to the European charged particle environment as ionospheric and pick-up ions. JEM composition
349 measurements must be able to find endogenic materials amidst the background of magnetospheric species
350 constantly raining down on the surface. JEM magnetic field measurements will have to retrieve the 3-D
351 picture of the four contributions to magnetic field configuration produced by the European magnetospheric
352 interaction: (1) the background undisturbed Jovian magnetic field, which is on the order of 450 nT; (2) a
353 never detected hypothetical intrinsic European magnetic field generated by a core dynamo mechanism, of
354 which we know only an upper limit (Schilling et al., 2004). Continuous low-altitude measurements by
355 JEM will decrease its detection threshold by at least an order or magnitude; (3) the magnetic fields
356 produced in the European environment by the European magnetospheric interactions; (4) the magnetic
357 effects of the electric currents induced into Europa's conducting ocean by the varying Jovian magnetic
358 field, on the order of 50-100 nT, which constitute a natural magnetic sounding of the ocean. To achieve a
359 good accuracy in this magnetic sounding of Europa's ocean, one must separate the Jovian source (1) and
360 the oceanic response to its variations (4) from the other two components. This goal can be achieved using
361 models of various levels of complexity, such as the MHD model by Blöcker et al. (2016), illustrated in
362 Figure 7. For the analysis of JEM magnetic field and plasma data, a comprehensive model separating the
363 four contributions and simultaneously constraining ocean thickness, conductivity, and atmospheric
364 densities will be developed, based on the data assimilation techniques currently used in meteorology and
365 related research areas. This inversion process will take advantage of the two-point magnetic field
366 measurements, on the orbiter and during the 22 days of operation of the lander at the surface.

367 Figure 7, which shows the current systems, the global distribution of ionospheric densities around Europa,
368 and the corresponding ionospheric currents, suggests that an orbit around 100 to 200 km altitude will
369 provide a good access to the current system near its intensity maximum.

370 Finally, the JEM orbiter would collect more useful data in two days of operation than what will be
371 obtained from Europa Clipper in 40 flybys spread over three years. If a continuous time series is available
372 from an orbiter for a period of 3 months or longer, one can use not only the main prime frequencies with
373 large amplitudes, but also the broadband spectrum of much weaker lower frequencies to sound the ocean

374 under the ice sheet. As shown in Figure 8, adapted from Khurana et al. (2009), these frequencies,
375 materialized by pink, green and yellow curves, allow a much better coverage of the (ocean thickness vs.
376 amplitude of the magnetic response) parameter space than the sole dominant frequencies at the 11.1 hr
377 (Jovian synodic) and European orbital (85.2 hrs) periods.

378 In addition, if the lander carries a magnetometer, simultaneous measurements with the orbiter will
379 facilitate the decomposition of the internal and external fields directly in time domain. The decomposed
380 internal and external field time series can then be Fourier decomposed into the primary field and Europa's
381 response at not only the two prime frequencies but also the weaker non-harmonic frequencies. A strong
382 advantage of two-point measurements is that even relatively short time series can be inverted into their
383 constituent primary and secondary fields.

384 In conclusion, JEM will perform the following investigations to address the PSO#1:

- 385 - Determine the global structure of magnetic fields, electric currents, plasma and energetic populations
386 in the European environment;
- 387 - Separate the four contributions to European magnetic fields and current systems;
- 388 - Use the natural fluctuations of the Jovian magnetic field to perform a broad-band magnetic sounding
389 of the European sub-surface ocean;
- 390 - Determine the composition/flux of plume material to characterize the properties of any subsurface
391 water.

392 **PSO#2: Determine the global structure of the solid body and potential biosphere of Europa, and**
393 **their response to Jupiter System tidal forcing.**

394 To achieve the measurement objectives of PSO#2, JEM will combine altimetry, gravimetry, the
395 characterization of rotation and magnetic measurements, using the geophysical investigations available on
396 the orbiter and on the lander geophysical station, with the additional support of astrometry measurements.
397 The following parameters will be determined in priority: (1) the harmonic expansion of the static gravity
398 field and of the topography up to degree 30-40, (2) the amplitude (precision $< 10^{-2}$) and phase (precision $<$
399 1°) of the gravity variations (k_2 Love number) and topographic deformation (h_2 Love number) of the
400 European tides, from which an accurate estimator of the ice shell can be derived, (3) the libration and
401 rotation properties of Europa, from radio science (gravity field), altimeter data and surface lander
402 positioning, (4) the instantaneous orbital characteristics of Europa and its long-term evolution, using the

403 PRIDE-E astrometry experiment analyzed in the context of previous astrometry measurements of the
404 orbital dynamics of the Galilean satellites (space and ground-based).

405 By combining these measurements, a rich set of integrated information on Europa's internal structure,
406 dynamics and energy budget will be produced, including: (1) detailed radial profiles of the key
407 geophysical quantities, (2) an assessment of the assumed hydrostatic equilibrium, (3) a global description
408 of the undulations of the critical interfaces: ice shell/ocean, ocean/rock mantle, rock mantle/core (if the
409 latter is precisely defined); (4) an accurate description of tidal deformation and heating, possibly
410 including constraints on its distribution between the different layers.

411 Figure 9 shows results of simulations we performed of the use of the gravity science investigation of
412 JEM. These results show that the gravity field can be retrieved up to a degree l of 30 and possibly 40 for
413 the orbital parameters and mission duration foreseen for JEM (compared to $l < 20$ for the 45 fly-bys of
414 Europa Clipper). Furthermore, the expected uncertainty on the measurement of Love number k_2 would be
415 about 20 times smaller: while Europa Clipper will do an excellent job to go beyond Galileo, significantly
416 augmented information about the interior of Europa will be provided by JEM.

417 Furthermore, the combination of the measured gravity and topography tidal waves will provide a direct
418 evaluation of the total ice shell thickness at the 5-km precision and of some of its mechanical properties at
419 the resolution necessary to provide key constraints for dynamic models of the ice shell, for instance to
420 decide about its conductive or convective nature. The combination of gravity and surface deformation
421 phase lags will further allow to discriminate between predominant tidal dissipation in the ice shell or in
422 the rock mantle, an important ingredient to investigate the coupling between the orbital dynamics and the
423 thermal evolution of Europa and better constrain the chemical coupling and mass transfer processes at
424 work between ocean, silicate floor, ice shell and surface.

425 PSO's 1 and 2 combined will provide unique information on the internal structure, layering and dynamics
426 of Europa, using the synergies between measurement techniques deployed on the orbiter and on the
427 lander. Figure 10 illustrates this complementarity of techniques (rotation monitoring, electromagnetic
428 sounding, gravimetry, seismic or acoustic sounding...) and shows how their combination will provide a
429 comprehensive description of key characteristics of the different layers of Europa's interior.

430 **2.2. Medium scale study: Determine the characteristics of the potential habitable zone of Europa.**

431 **PSO#3: Understand the exchange and transformation processes at the interface between the ice-**
432 **shell surface/subsurface and the exosphere/ionosphere including potential plume characterization**

433 Europa's surface and exosphere. Europa's surface is composed of an icy porous regolith (50 to 100 μm
434 grains) permanently bombarded by Jovian magnetospheric energetic ions (essentially keV to MeV $\text{S}^{\text{n}+}$ and
435 $\text{O}^{\text{n}+}$ coming from Io's torus) and electrons (equivalent of 100 to 1000 times the dose rate at the Moon) and
436 by photons (Cooper et al. 2001). The radiolysis and photolysis induced by this bombardment alter the
437 optical layer of the surface, from microns up to meter depth, on a time scale between 10 and 10^9 years.
438 The typical yield of S^+ and O^+ at keV to MeV energy is around 1000, so that the ice resurfacing rate
439 induced by sputtering should be of ~ 0.1 microns / year (or 100 m/Gyr), significantly lower than the
440 resurfacing rate due to meteoroid. As a consequence, the regolith can be a substantial trap for radiation-
441 altered material.

442 The incident magnetospheric particles and photons decompose Europa's icy surface into H_2 , O_2 and H_2O_2 .
443 Preferential loss of the volatile H_2 leaves an oxidized surface, a gravitationally bound O_2 atmosphere and
444 peroxide trapped in ice (see the right-hand side of figure 11 from Shematovich et al. 2005). This
445 processing also determines the state of trace species such as S, C, Na, K and Mg. Sources and sinks of
446 trace species in Europa's icy surface are: implantation from Io plasma torus, upwelling or venting from
447 interior sources, and meteorite impacts. As a result of sputtering, Europa's exosphere is expected to
448 display a composition closely related to the surface composition, thus providing a probe to understand
449 how the surface composition is processed by radiolysis/photolysis, enriched by exogenic sources and
450 eroded by sputtering. The ultimate goal for JEM will be to estimate the respective role of these processes
451 and their spatial and temporal variations, using three signatures for each of these processes:
452 compositional, energetic and spatial.

453 Europian plumes. Based on Enceladus studies, Europian plumes might be stratified according to the
454 density of materials, with dust grains of salt, silicate materials or heavy organics remaining in the lower
455 parts of the plume, while light volatiles would reach higher altitudes. Thus, the compounds that could be
456 analysed at different altitudes could provide information about the formation history and habitability of
457 the moon.

458 In summary, JEM will perform the following investigations in the context of PSO#3:

- 459 - Determine the composition and spatial distribution of major and trace species of Europa's exosphere;
- 460 - Ascertain the roles of the surface/subsurface, magnetosphere, dust and possibly plumes as drivers of
461 exosphere formation.

462 **PSO#4: Understand the exchange processes between the ice-shell surface/subsurface and the**
463 **potential habitable zone.**

464 Exchange processes between the ice-shell surface/subsurface and deep aqueous layers constrain the
465 possibility of finding signatures of the non-accessible habitable zone with JEM observations of surface
466 and subsurface chemistry and geological features. The extreme diversity of these surface features is
467 illustrated in Figure 12. In order to recognize which features are young and have endogenous origin, JEM
468 will benefit from: a) Europa Clipper and JUICE mission measurements of remote imaging, spectroscopy
469 and radar scanning of Europa, which will provide for the first time detailed information on geological
470 features, activity and history at regional resolution; b) JEM global accurate geophysical measurements,
471 particularly topography; c) JEM novel information at the local scale of the landing site.

472 Resurfacing by cryovolcanism, geyserism or tectonism could have effects on transportation of materials
473 and cycling of the elements in the moon. In this regard, the study of the local geological features (e.g.
474 morphology, grain sizes of surface materials, presence of boulders, presence of small craters, stratigraphic
475 relationship between materials), the distribution of materials, and the subsurface structure at the landing
476 site will help to characterize the nearest aqueous layer at the lander spot. A relation between surface and
477 subsurface features can reveal the depth of liquid reservoirs and their putative links to the surface.

478 Due to the extreme conditions on the surface, the relative abundances of key materials for habitability,
479 such as organics, minerals and volatiles containing bio-essential chemical elements might differ according
480 to their stratigraphy position, chemical state (redox state, degradation rate) and phase (e.g. water
481 ice/clathrate hydrate). Deposition of radiation energy into materials is controlled by the chemical and
482 physical properties of the regolith at the landing site (e.g. grain size, porosity mineral, crystallinity). These
483 parameters determine the so-called “biosignature preservation potential” (BPP) at the surface/subsurface,
484 which is especially significant for the search for biosignatures (see 2.3). Magnetic field intensity and
485 radiation dose measurements at the landing site will be needed to determine the BPP. Selection of the
486 landing site is critical to maximize the probability of finding fresh endogenous materials, which seems to
487 be more frequent in the leading hemisphere according to previous studies (see Figure 13).

488 Availability of chemical elements that life needs depends on the physical and chemical properties of the
489 solvent. This novel investigation can be performed by JEM by characterizing the melt endogenous
490 materials in the liquid state: a) pH, since it influences the stability, reactivity and mobility of elements,
491 inorganic and polar organic compounds; b) Redox potential, which affects the behavior of many elements
492 and chemical constituents in aqueous media and in the living organisms and is the main energy source for
493 chemotroph organisms; c) conductivity, which is affected by salinity. Dissolved inorganic ions such as

494 Mg^{2+} , Ca^{2+} , K^+ , Na^+ , Cl^- , SO_4^{2-} , HCO_3^- and CO_3^{2-} can constitute redox couples that could provide energy
495 for chemosynthetic life; d) volatiles (e.g. CH_4 , NH_3 , O_2 , H_2) that are sources of nutrients and potential
496 biosignatures.

497 In summary, the investigations that JEM will perform to address PSO #4 are:

498 - Detect any geological feature which involves exchange processes between surface/interior at the
499 landing site and determine whether any activity exists today;

500 - Determine the proximity to liquid water reservoirs in the landing site area;

501 - Characterize the biosignature preservation potential of accessible surface materials at the landing site;

502 - Characterize the physical properties at the landing site;

503 - Characterize the key compounds associated with habitability near the surface;

504 - Characterize the wet context of surface materials.

505 **2.3. Local scale study:**

506 **PSO#5. Search for bio-signatures at the surface / subsurface.**

507 At present, space exploration considers distinct categories of biosignatures requiring different analytical
508 techniques with different detection limits:

509 1) General biomarkers (molecular bio-signatures) are indisputable evidence of life. They are biological
510 polymers like polysaccharides, lipids, proteins or some form of information-transmitting molecule similar
511 to DNA. Of particular interest are conservative biomolecules that are deeply and ubiquitously rooted in
512 the tree of life, proteins that are involved in deeply rooted and widespread metabolic pathways, structural
513 components of cell walls of broad prokaryotic groups, and phylogenetically conserved structural proteins
514 and storage compounds of broad prokaryotic groups conserved under stress, e.g. with limited water
515 availability. These different groups are presented in Figure 14.

516 2) Organic indicators of past or present life. Since high radiation conditions on the European surface may
517 degrade any material if it is exposed for any length of time, biomolecules will likely break up and react,
518 producing degraded organic compounds that can also be symptomatic of the presence of life. It is critical
519 to validate the biological origin of those degraded compounds.

520 3) Inorganic indicators of past and present life: biogenic stable isotope patterns in minerals and organic
521 compounds, biogenic minerals, or certain atmospheric gases produced by metabolism.

522 4) Morphological and textural indicators of life, e.g. any object or pattern indicating bio-organic
523 molecular structures, cellular and extracellular morphologies, or biogenic fabric on rocks.

524 Discerning the origin of the bio-signatures is mandatory, specifically for the simpler organics since they
525 may as well come from meteorites or from ejecta produced by plume activity. Organics may form by
526 interaction of surface materials with the radiation environment if CO₂ is originally present in the ice
527 matrix (Hand et al., 2007). Detection of formamide (CH₃NO) is particularly crucial, since it is a key
528 compound for the formation of nucleic acids. However, an exogenous origin of some organics (e.g. PAH)
529 cannot be ruled out.

530 The JEM search for biosignatures will primarily focus on local scale studies on a landing site where fresh
531 and young material will be expected, coming from the near surface or even from putative plumes. In near-
532 surface investigations, direct sampling and contact analysis instruments are absolutely necessary since the
533 concentration of bio-signatures is assumed to be very low. Sampling materials at depths below 5-10 cm
534 from the leading hemisphere is required for access to unaltered molecules. Measurements may require the
535 sample to be in the solid or liquid phase for analysis, depending on the biosignature typology and the
536 technique used for its recognition. Simple molecules of categories 2 and 3 can be detected and identified
537 directly by vibrational spectroscopy if they are present in the solid matrix of ice. For isotopic ratios and
538 some more complex organics (e.g. amino acids, lipids), their unambiguous identification can be
539 performed by mass spectrometry after sample volatilization, which is a step of the GC/MS procedure. To
540 unambiguously identify macromolecules of category 1 (e.g. polysaccharides, proteins or DNA/RNA) a
541 biochemical analytical technique is necessary, such as antibody microarrays immunoassays. This
542 technique can identify macromolecules because they bind to their particular 3D structures in a liquid
543 medium, which is needed to transport the antibodies and to allow binding to the specific antigens/target
544 molecules. In JEM, the liquid medium will be obtained by melting the ice sample of the near surface.
545 Antibodies can also recognize and identify small but still complex molecules such as aromatic amino
546 acids (Phe, Tyr, Trp) and PAHs such as benzo-a-pyrene.

547 Besides near-surface science, JEM will also search for bio-signatures of extant life in the exosphere and
548 in plumes if their existence is confirmed. Traces of life there could include organic and inorganic
549 biosignatures expelled from the habitable zone, even cells, cellular material, or biomolecules. Closer to

550 the “vent” exit points, deposits containing rock fragments hosting either extant (or recently dead) life
551 forms or the fossilized remains of life might be found.

552 In conclusion, PSO #5 will include a set of investigations which are unique in the Solar System
553 exploration, such as:

554 - identifying general biomarkers;

555 - detecting and characterizing any organic indicator of past or present life;

556 - identifying morphological and textural indicators of life;

557 - detecting and characterizing any inorganic indicator of past and present life;

558 - determining the origin of sampled material;

559 - determining if living organisms persist in sampled materials.

560 **3. Proposed scientific instruments:**

561 The implementation of the JEM science plan is based on the joint operation of scientific investigations on
562 two complementary platforms: a lander (currently under study by NASA) and a carrier/orbiter, each
563 including a baseline main element and an optional small detachable platform. We describe now the
564 instrument suite required on each of these platforms to meet our measurement requirements.

565 **3.1. The Orbiter instrument suite.**

566 To meet our measurements requirements, we propose that the Orbiter carries the instruments listed in
567 Table 1, some of them to be operated during a minimum of 22 days simultaneously with lander data relay,
568 then all of them during the subsequent 3 months of nominal orbital science, and again some of them
569 during the final descent to Europa’s surface. The added complexity of the extreme radiation environment
570 at Jupiter drives the orbiter instrument architecture. We make the choice of decoupling the sensor heads
571 from their part of their electronics. This allows flexibility in their accommodation, easier radiation
572 mitigation, full integration of the scientific capabilities of each of them and ensures optimum science
573 return while keeping the total resources low.

574 The gravity field, the tidal deformations (both gravitational and physical) and the rotational state
575 (obliquity and physical librations in longitude) will be determined by means of Doppler and range

576 measurements carried out both on the orbiter-to-ground, two-way, coherent link, and on the orbiter-to-
577 lander proximity link. The two-way link to ground, enabled by an onboard transponder (Integrated Deep
578 Space Transponder or IDST) operating at X or Ka-band, will provide radiometric observables to estimate
579 a $> 20 \times 20$ gravity field, k_2 Love number, and global obliquity and physical librations of the moon.

580 The magnetometer (MAG) instrument will measure the magnetic field in the vicinity of the spacecraft.
581 This is crucial for a) resolving the interaction of Europa with Jupiter's magnetosphere with multipoint
582 measurements, b) constraining the extent of Europa's intrinsic magnetization, and c) searching for
583 evidence of induced electric currents in Europa's subsurface ocean. The typical range, resolution, and
584 noise-level of this instrument are $\pm 10 \mu\text{T}$, up to 50 pT (dependent on range), and $< 100 \text{ pT}/\sqrt{\text{Hz}}$ (at 1 Hz)
585 respectively. The range is more than adequate to measure expected magnetic fields at Europa.

586 The Laser Altimeter (LA) will investigate the surface and interior of Europa. By measuring the time-of-
587 flight of a laser pulse transmitted from the instrument, backscattered at the moon's surface and detected in
588 the instrument's receiver telescope, height profiles can be obtained in along-track direction. Combining
589 many of these tracks, the local, regional, and global topography of Europa can be obtained. From the
590 pulse-spreading of the returned pulse the surface roughness on the scale of the laser footprint (order of a
591 few tens of meters) can be measured. Information on the albedo at the laser wavelength (1064 nm) can be
592 gained from the intensities of the transmitted and returned pulses. By obtaining not only good spatial
593 coverage but also temporal coverage with laser ground-tracks, the tidal deformation of Europa's ice shell
594 along its orbit around Jupiter will be measured. From the tidal signal (expressed in terms of the radial
595 tidal Love number h_2), the extension of Europa's ice shell can be constrained, especially when combined
596 with measurements of the tidal potential by the radio science experiment. By measuring the phase-lag of
597 tidal deformation LA will provide constraints on the internal heat production of Europa. Combined with
598 phase-lag measurements of the tidal potential a highly dissipative silicate interior could be detected. The
599 instrument is composed of a transceiver unit and two electronic units. The transceiver unit contains the
600 complete laser subsystem and the optical chain of the receiver.

601 The Ion Mass Spectrometer and Electron Spectrometer (IMS/ELS) suite will provide the most
602 comprehensive and critically needed thermal and suprathermal plasma measurements to achieve the
603 following science objectives: (1) reliably characterize plasma ion and electron currents constituting major
604 backgrounds for magnetometer detection of the oceanic source of induced magnetic field; (2) characterize
605 Europa's environment, its composition, structure and dynamics and Europa's interaction with the Jovian
606 magnetosphere; and (3) unveil and quantify the key processes of erosion and exchange of elements at

607 Europa surface, including presence of expelled minor/trace elements, possibly representative of sub-
608 surface layers.

609 The ELS sensor is an electrostatic analyzer that will provide fast 3D measurements in the energy range 1
610 eV-30 keV and will be customized for the energy range as well as the dynamic range encompassing
611 magnetospheric suprathermal and thermal plasma originating from Io, cold ionospheric species including
612 photoelectrons and ram negative ions from Europa, as well as pick-up negative ions likely to be observed
613 around Europa.

614 The Ion Mass Spectrometer (IMS) sensor is a 3D mass spectrometer that will measure positive ion fluxes
615 and provide detailed composition measurements at Europa. A major feature of IMS is its Time Of Flight
616 (TOF) section, which includes two MCP detectors, one with high-count measurements to ensure a good
617 time resolution, and a second one, based on the reflectron technique, to provide an enhanced mass
618 resolution. This double detection allows a detailed composition analysis capable of measuring multiply
619 charged ions and separating ions of the same mass / charge ratio (e.g. S⁺⁺ and O⁺).

620 The Ion and Neutral Mass Spectrometer (INMS) is a time-of-flight mass spectrometer using an ion mirror
621 (reflectron) for performance optimization. A TOF mass spectrometer has inherent advantages with respect
622 to other mass spectrometer concepts since it allows recording of a complete mass spectrum at once
623 without the necessity of scanning over the mass range of interest. INMS is a time of flight (TOF) mass
624 spectrometer with $M/\Delta M \approx 1100$ resolution over a mass range of $M/q = 1-1000$ u/e.

625 The Dust Analyzer (DA) is a TOF impact mass spectrometer that uses the technology of the successful
626 Cosmic Dust Analyzer (CDA) operating on Cassini and employs advanced reflectron-type ion optics
627 optimized for the combination of high mass resolution, large target area, and large Field-of-View (FOV).
628 For unambiguous recognition of valid dust impacts, a coincident detection method will be implemented
629 with all analog signals being continuously monitored with threshold detection.

630 The additional Langmuir Probe (LP) (if resources allow it) will consist of one boom with a spherical
631 sensor at the tip. The LP will monitor the cold plasma parameters (electron and ion number densities, the
632 electron temperature and the plasma drift velocity), as well as signals from micrometeorite impacts on the
633 S/C. The derived LP parameters will provide the basis to a) characterize the European ionosphere and its
634 dynamics; b) characterize the plume dust and plasma properties; c) characterize the ambient size/mass
635 distribution of mm-sized dust around Europa and in the Europa torus; and d) monitor the spacecraft
636 potential for use by the particle spectrometers and for the determination of the integrated EUV flux.

637 In addition, the Planetary Radio Interferometry and Doppler Experiment for JEM (PRIDE-E) is an
638 instrument with zero demand on the science payload mass, and only ad hoc demand on other S/C
639 resources (the onboard power, commands, telemetry). This experiment is designed as an enhancement of
640 the science output of the mission using the JEM radio links and the extensive infrastructure of Earth-
641 based radio astronomy facilities. PRIDE-E is a repetition of PRIDE-JUICE, one of the experiments of the
642 JUICE mission (Witasse et al. 2015). PRIDE is based on the use of Very Long Baseline Interferometry
643 (VLBI) instrumentation available and operational on more than 40 Earth-based radio telescopes. The
644 applicability of the VLBI technique for ad hoc experiments with planetary probes has been demonstrated
645 for the Huygens probe (Pogrebenko et al. 2004, Lebreton et al. 2005, Bird et al. 2005), Venus Express
646 (Duev et al. 2012., Bocanegra Bahamón et al. 2018) and Mars Express (Duev et al. 2016, Bocanegra
647 Bahamón et al. 2019) missions. The prime scientific objective of PRIDE-E is to provide inputs into
648 improvement of the ephemerides of the Jovian system. PRIDE-E will also provide complementary
649 measurements of the S/C lateral coordinates and radial velocity in the interests of other science
650 applications. Various applications of PRIDE-E measurements for improvements of Jovian system
651 ephemerides and related parameters are discussed in detail by Dirkx et al. (2016, 2017, 2018).

652 To accommodate and operate this instrument suite on the Orbiter Science Platform will take the estimated
653 resources shown in Table 2.

654 3.2. The Lander instrument suite.

655
656 On the NASA side the instrumentation for the lander will be selected based on a future AO to which
657 European institutes may contribute under the umbrella of their national funding agencies. In this section
658 we focus on the sensors to be delivered by ESA to the lander through the proposed standalone
659 Astrobiological Wet Laboratory (described in section 4.3.3) augmented by two geophysical sensors. To
660 meet our measurements requirements, the Lander should carry the instrument suite presented in Table 3,
661 to be operated during a minimum of 22 days.

662 Multi-probe immunoassay-based (MPAS) instruments have been proposed for planetary exploration: the
663 Life Marker Chip (LMC) (Sims et al, 2005; 2012) and the Signs Of Life Detector (SOLID) (Parro et al.,
664 2005; 2008; 2011), but neither LMC nor SOLID can be implemented in the AWL because of mass and
665 volume restrictions. We are therefore proposing a different approach adapted to AWL constraints.

666 The MPAS instrument must be based on simplicity and robustness. It minimizes the use of electronic
667 devices, mechanical actuators and power consumption. The most promising concept is something well

668 known on biomedical laboratories: the lateral flow assay (LFA) or immunocapillary test, as it is also
669 called. The first immunoassay based on lateral flow was reported in 1978 and it has been extensively used
670 on pregnancy tests (Mark, 2010). In the LFA developed for MPAS, the *Sample Pad* is in contact with the
671 fluid deposit and it is flooded with the water sample coming from the ice fusion. The sample moves
672 forward by capillarity to the *Conjugate Pad*, preloaded with a set of antibodies (Ab) labeled with colloidal
673 gold or colored latex spheres. At this step the target molecules (organics, biomarkers, or antigen-Ag) bind
674 to their corresponding Ab's and the sample movement continues through the *Detection Pad*. Once the
675 labeled sample gets the multi-probe *Detection Array*, the couple Ag-Ab binds again to the immobilized
676 Ag-conjugate (in a competitive immunoassay) or immobilized capturing Ab (sandwich assay), and dark
677 spots corresponding to the trimeric complexes Ag-AuAb-ConAg or Ag-AuAb-capAb are visualized by
678 illuminating (visible) the array and image capturing with a small camera.

679 The Multiparametric probe (MPP) will have heritage from the MECA package onboard the Phoenix
680 mission which was the unique probe with capability to perform chemical analysis of a water sample. The
681 MECA package (Kounaves, 2003) was a wet chemistry lab with sensors to measure: H⁺, dissolved O₂,
682 redox potential, oxidants and reductants, and several ions and cations. The MECA package was designed
683 as a multi-sample instrument with a mass, volume and power consumption out of the scope of the
684 instrumentation for this mission. From the different alternatives available in the environmental monitoring
685 market, the most attractive by its miniaturization capabilities are those sensors based on ChemFET
686 technology (Jimenez-Jorquera, 2010). Oxygen dissolved, pH, conductivity, NH⁺, NO³⁻, Ca²⁺, K⁺, Cl⁻, NO³⁻ are
687 parameter with sensors developed to measure it.

688 The VISTA (Volatiles In Situ Thermogravimetric Analyzer) sensor is a miniaturized thermogravimetry
689 analyzer that will perform measurements of the Europa volatile compounds (Palomba et al. 2016). The
690 instrument is based on thermogravimetric analysis (TGA) and its core is a Quartz Crystal Microbalance
691 (QCM), oscillating at a resonant frequency linearly related to the mass deposited on its sensible area. The
692 technique measures the change in mass of a sample as a function of temperature and time. VISTA
693 measurement goals are: a) to discriminate between water ice and clathrate hydrates, by heating the QCM
694 up to the decomposition temperature of clathrate hydrates at 120-160 K (Lunine and Shevchenko 1985)
695 and to the sublimation temperature of water ice (200 K at a depth of 3 meters, Handbook of Chemistry
696 and Physics 1980), and by recording the temperature at which mass loss due to heating occurs; b) to
697 measure the composition of non-ice materials, by heating the PCM up to the dehydration temperatures of
698 possible Europa components, ranging in the interval 220-320 K (McCord et al. 2001), by recording the
699 temperature where mass loss due to heating occurs and by measuring the volatile/refractory abundance
700 ratio (this measurement which is fundamental to characterize the non-ice material is not performed by

701 other instrumentation onboard the lander); c) to detect and measure the relative abundance of organics, by
702 heating the PCM up to organics desorption at about 230 K (Chazallon et al. 2004), and by measuring the
703 mass difference before and after desorption.

704 The magnetometer can provide magnetic field measurements at a rate of up to 128 Hz and an accuracy of
705 0.1 nT. One on the lander itself, and one on a short (0.5m) boom will ideally be needed. The laser
706 retroreflector has the property to reflect light back to its source with a minimum of scattering. A laser
707 onboard the orbiter could target the device from a distance of tens to hundreds of thousands of km (for
708 instance from the halo orbit). Attached to the lander it would allow to determine the exact landing site
709 with a precision of a few meters and the measurement of tides and of the rotational state already during
710 the relay phase (like a control point). The device is fully passive (no power or data consumption). A good
711 example is the ExoMars 2016 Schiaparelli retroreflector ([http://exploration.esa.int/mars/57466--
712 retroreflector--for--exomars--schiaparelli/](http://exploration.esa.int/mars/57466--retroreflector--for--exomars--schiaparelli/)). It has a size of 54 mm in diameter and a total mass of 25 g.
713 Our estimate of the resources needed to operate this instrument suite on the Surface Science Platform is
714 shown in Table 4.

715 **4. Proposed mission configuration and profile**

716 **4.1. JEM orbits and science operations.**

717 The implementation of the science plan of JEM will rest upon instruments deployed synergistically on
718 two space platforms: a carrier/relay/orbiter platform (hereafter referred to as orbiter), and a soft lander
719 platform, both described in section 4.2. These 2 platforms will be used to perform the 3 sequences of
720 scientific observations, or **science sequences**, illustrated in Figure 15:

721 **A. A surface science sequence** involving the lander instruments, planned to last about 22 days on a
722 selected site;

723 **B. An orbital science sequence** involving the orbiter instruments. This sequence will first overlap
724 in time with the surface science sequence, while the orbiter platform will reside on a halo orbit of
725 the Jupiter-Europa system to relay the orbiter data to Earth, before continuing in low European orbit
726 for a planned duration of three months;

727 **C. A descent science sequence** will correspond to an additional period, after the end of sequence
728 B, during which the orbiter will explore regions of the exosphere/ionosphere very close to the
729 surface, below the lowest altitude to be covered by Europa Clipper, to search for biomolecules in
730 the lowest layers of the exosphere.

731 Our astrometry experiment PRIDE-E (section 3.4), will support and complement these three sequences
732 from Earth using the world-wide VLBI network of radio telescopes.

733 The determination of the landing site (sequence A) and of the B and C orbits must be the result of a
734 detailed optimization aimed at fulfilling our measurement requirements. For sequence B, we have chosen
735 a scenario fulfilling different requirements on two different successive orbits. For sequence C, the
736 requirement of measuring exospheric species in the near-surface exosphere could be implemented by de-
737 orbiting the orbiter platform and taking data from its initial orbit until final impact, or by letting the
738 working orbit of sequence B evolve naturally until final impact. A detailed mission analysis will be
739 needed to identify the most promising approach.

740 The spatial/temporal coverage provided by our JEM orbiter will nicely complement the coverage and the
741 scientific information to be provided by Europa Clipper, which will have flown 45 times by Europa a few
742 years before JEM, providing data both much closer to the surface, and at much larger distances from it,
743 than the high-inclination orbits of JEM will allow. JEM will provide a three-months continuous coverage
744 of European planetary fields and plasma populations on a high-inclination orbit, after an initial sequence
745 on a halo orbit which will provide a detailed insight into the structure of the European Alfvén wings. To
746 reach these orbits, starting from Earth with a SLS launch, the JEM flight complement will have to go
747 through a succession of mission sequences (S-1 to S-9) listed in Table 5, first on heliocentric orbits and
748 then on Jovicentric orbits before reaching its first European orbit.

749 The choice of the sequence of orbits will be the result of a trade-off in a 3D parameter space described by:

750 - the Total Ionizing Dose (TID) accumulated along the spacecraft trajectory, which gives the maximum
751 operation time our platforms will be able to live through;

752 - the shielding thickness used to protect the equipment and mitigate radiation dose effects, which has a
753 direct incidence on the weight of the platform and instruments;

754 - the total Delta V provided by the propulsion system, with direct impact on spacecraft total wet mass.

755 The JEM spacecraft will first cruise on a DV-EGA trajectory to Jupiter (Figure 16, sequence S-1). We
756 choose this trajectory to bring the maximum mass possible into Jovian orbit and accommodate a
757 significant science payload on each platform, at the expense of a larger travel time.

758 After a Jupiter Orbit Insertion (JOI) immediately followed by a Perijove Raise Manoeuvre (PRM) to
759 minimize exposition to the inner parts of the Jovian radiation belt (sequence S-2), the JEM spacecraft will

760 execute a tour in Jovicentric orbits to reach Europa (sequence S-3 and figure 17). Here we choose the 12-
761 L1 tour with only flybys of two Galilean satellites (Ganymede and Callisto) to reach Europa in a short
762 time and minimize the dose accumulated (Campagnola et al, 2014), in order to enable a lifetime in
763 European orbit significantly above 4 months, at the expense of a significant Delta V. At the end of
764 sequence S-3, the JEM flight complement is injected on an eccentric European orbit from which the lander
765 stack is released, de-orbits and executes its landing sequence.

766 Immediately after lander release, the JEM orbiter will be transferred to a halo orbit to fulfil its relay
767 function. At that point, the lander and the orbiter will start their science operations.

768 The geometry of the science orbits has been the object of a mission analysis summarized in Annex III. It
769 is shown in Figure 18. During the 35-day surface science sequence, the orbiter is primarily used to study
770 the Alfvén wings produced by the European magnetospheric interaction (sequence S-5). At the end of
771 surface science operations, it is transferred to a low altitude 200-km high-inclination orbit to perform a
772 global mapping of gravity and magnetic fields and of the European plasma populations (sequence S-7).
773 After 3 months of science operations, the orbiter leaves its 200-km circular orbit to explore the very low
774 latitude exosphere in the final descent sequence (S-8).

775 **4.2 Environmental constraints on the JEM mission**

776 Planetary protection:

777 As the interest in icy Solar System's bodies is increasing with exciting new findings, new missions are
778 proposed and particularly towards Jupiter's moon Europa. On the basis of deliberations of the dedicated
779 Task Working Group on the Forward Contamination of Europa (NRC, 2000) and of the studies of new
780 international experts working groups such as the "Planetary Protection for the Outer Solar System"
781 (PPOSS) working group commissioned by the European Science Foundation, a conservative approach has
782 been defined to be required to protect the European environment: Indeed since Europa may have a global
783 ocean possibly connected with the surface, viable extremophile microorganisms such as cold and
784 radiation tolerant organisms may survive a migration to the sub-surface of the ocean and multiply there.
785 According to the COSPAR Planetary Protection policy, a general requirement for every lander mission to
786 Europa, categorized as IV, has to be applied in order to reduce the probability of inadvertent
787 contamination of a subsurface ocean by viable terrestrial microorganisms or their spores to less than $\sim 10^{-4}$
788 per mission (1 viable microorganism / 10,000 missions).

789 COSPAR Planetary protection policy of Icy moons missions is under revision. In the context of future
790 missions to these moons, some concepts require an updated definition such as: the environmental

791 conditions potentially allowing terrestrial organisms to replicate; the specific problematic species that
792 might easily adapt to such extreme environments; the period of biological exploration of 1000 years
793 already discussed for Europa Clipper; and even a definition and characterization of "Enhanced Downward
794 Transport zones" at the surface of icy moons that require special care (Coustenis et al., 2019).

795 In the case of the Europa lander, there is a consensus that planetary protection requirements must be even
796 more stringent than for Mars. The NASA Europa Lander team, following the previous requirements
797 defined for Europa Clipper, proposes changes in the entry parameters used to calculate the probability of
798 contamination of the European surface/subsurface. As examples of this severity, all species in the
799 bioburden should be included, not just bacterial spores, and the probability of contaminating a liquid
800 reservoir with less than 1 living organism should be estimated. To achieve that, new approaches and
801 technologies must be implemented, such as terminal sterilization systems and lethality modelling
802 including bio-reduction due to spaceflight.

803 In order to comply with these significantly more stringent International Regulations and to meet the
804 maximum allowed bioburden levels, a strict planetary protection strategy will be set up for JEM. It will
805 integrate the lessons learnt from the past, current and planned missions to the outer Solar System,
806 including those regarding the limitation on crash probability for orbiters, the sterility requirements on
807 landers, penetrators and orbiters that do not meet the non-crash probability, and an ultra-cleanliness level
808 for all life detection instruments and those which are not exposed to the sterilising radiation during the
809 spaceflight.

810

811 Radiations:

812 The inner magnetosphere of Jupiter where Europa orbits is the most severe radiation environment in the
813 Solar System. This presents significant challenges for operating a spacecraft and its science instruments at
814 Europa. The phases when the mission elements are in orbit around Europa are by far the most
815 constraining ones in terms of radiation doses. Low-altitudes orbits around Europa however have a clear
816 advantage in terms of reduced radiation doses when one takes into account the complex trajectories traced
817 by charged particles in the combined Jovian and European magnetic fields (Truscott et al., 2011). Figure
818 19 shows the results of our radiation analysis for these phases using SPENVIS, the JOSE model, as well
819 as various assumptions described in the caption. The sensitive parts and electronics will need to be
820 shielded to reduce the effects of the total ionizing dose (TID), which is equivalent to 50 kRad inside a 22
821 mm Al sphere. Table 6 presents the total ionizing doses received during the different phases of the Europa
822 science mission as a function of the thickness of the aluminium shield. A number of mitigation measures

823 in subsystems designs, shielding of critical elements, and use of radiation hardened parts are discussed in
824 sections 3 and 4.3.

825 Europa is within a hard radiation environment, with particle fluxes >20 times larger than at Ganymede.
826 The instantaneous background flux due to radiation in low-altitude Europa orbits presents significant
827 challenges for the science instruments but is slightly lower than the JUICE worst case. The flux is on the
828 order of up to 10^5 - 10^6 $\text{cm}^{-2} \text{sr}^{-1} \text{s}^{-1}$ behind 10-20 mm Al. This higher background may have a significant
829 impact on the SNR of certain detectors. Sophisticated background suppression techniques will need to be
830 implemented together with shielding optimizations in order to ensure maximal science return as discussed
831 in section 3.

832 **4.2. The JEM flight system.**

833 *Global architecture.*

834 In its baseline configuration, illustrated in Figure 20, the JEM flight system is composed of two platforms,
835 possibly augmented by an additional CubeSat element (Gaudin, 2016), not described in this article:

836 - **A soft lander platform:**

837 Given the heritage and expertise gained from previous studies, this platform, with 26 kg payload mass
838 class (including a 32% margin) operating 22 days on surface, should most likely be delivered by NASA
839 with possible contributions of European national agencies at the investigation level. It will perform
840 investigations in astrobiology, ice characterization and geophysics (Hand et al. 2017).

841 As an essential component of the JEM concept, we propose that ESA studies and discusses with NASA
842 the procurement of a small sub-platform, the «Astrobiology Wet Laboratory » (AWL), to conduct original
843 astrobiology investigations specialising in the analysis of wet samples (see 4.3.3).

844 - **A carrier/orbiter/relay platform:**

845 This platform will fulfil the key functions of injecting the lander stack into an European orbit just prior to
846 its de-orbitation, and of relaying the lander data to Earth. It will also carry a focused instrument suite
847 (section 3.1) to perform global high-resolution measurements of the gravity, magnetic field and
848 topography fields and of the plasma/neutral environment along European orbits.

849 **Optional augmentation:** a mission that is likely to fly beyond 2030 should include a small platform that
850 could be released from the main orbiter in European orbit to perform focused scientific measurements.
851 Following an open call to the academic community for cubesat ideas, it could be selected on the basis of
852 scientific merit, either as a science contribution to one of the JEM PSO's, or as an opening to a new
853 research theme. One particularly appealing option has been studied by the authors of this article: using a
854 cubesat for a targeted flyby through a Europa plume that would have been previously identified during the
855 beginning of the Europa science orbits (Gaudin et al., 2016).

856 **4.2.1. The JEM Orbiter complement.**

857 **4.2.1.1. The carrier / orbiter / relay platform**

858 The JEM carrier/orbiter platform will serve two objectives: (1) deliver the NASA lander to an orbit
859 around Europa, and relay its scientific data to Earth; (2) perform global high-resolution measurements of
860 the gravity, magnetic field and topography fields and of the plasma/neutral environment. The proposed
861 JEM orbiter concept, presented in Annex II, is inherited from two platforms currently developed by ESA:

862 1- the European Service Module (ESM) of the Orion Multi-Purpose Crew Vehicle (MPCV), from
863 which the mechanical and propulsion bus is adapted for JEM. The ESM serves as primary power and
864 propulsion component of the Orion spacecraft. It presents several advantages for the JEM mission: it can
865 carry a very heavy payload (the Orion Crew Vehicle is in the 10 tons class), it can be launched on SLS,
866 and it is developed in a NASA / ESA collaboration framework. Many key systems proposed to be reused
867 for JEM will be flight-proven at the time of JEM mission adoption.

868 2- the Jupiter Icy Moons Explorer (JUICE) platform, which provides a relevant basis for the avionics of
869 an interplanetary mission to Jupiter. The JUICE spacecraft, to be launched in May 2022, provides key
870 assets for the other components of the JEM orbiter: a rad-hard avionics adapted to the specific constraints
871 of an interplanetary mission and protected within a lead-shielded vault, and a power subsystem designed
872 for LILT (Low Intensity Low Temperature) conditions.

873 Figure 21 shows the general configuration of the carrier/orbiter and its interface with the lander stack,
874 before deployment (left) and just after lander stack release (right).

875 **4.2.2. The JEM Lander complement.**

876 **4.2.2.1. The Soft Lander platform.**

877 For the purpose of this work we assumed that the soft lander platform will be delivered by NASA and
878 benefit from the heritage of several previous studies of its concept. Figure 22 shows its architecture in the
879 2017 SDT report (Hand et al., 2017), a concept still under review. The soft lander will be the final
880 element of the “lander stack” which also includes a propulsion stage and a sky crane following a concept
881 similar to the Mars Science Laboratory sky-crane. A gimbaled high gain antenna, co-aligned with the
882 panoramic camera and mounted on the same articulated mast, will be used for the communications with
883 the carrier-orbiter. The lander will be equipped, in addition to the payload, with a robotic arm with
884 collection tools.

885 In line with the JEM science plan, we propose the functional structure presented in figure 23 for the
886 surface science platform carried by this soft lander. The analysis of samples of astrobiological interest
887 will be performed by two complementary sample analysis facilities, one devoted to the analysis of solid
888 samples, and another one dealing with liquid samples. The interest in the wet chemistry measurements is
889 testified by the recent selection in the ICEE-2 program for instrument development of two technologies
890 incorporating microfluidic systems (MICA: Microfluidic Icy world Chemistry Analyzer ; MOAB:
891 Microfluidic Organic Analyzer for Biosignatures). The two facilities will be served by a common
892 articulated arm shown in figure 22. In addition to astrobiology investigations, the lander will also operate
893 a geophysics station for the study of the planetary fields, the sounding of the sub-surface and the study of
894 the properties of the surface ice.

895 We propose that the liquid sample analysis facility, called AWL for Astrobiology Wet Laboratory, be
896 developed by ESA with sensor provided by its member states.

897 **4.2.2.2. The Astrobiology Wet Laboratory (AWL)**

898 We envisage two accommodation options for the AWL: on the lander (AWL/L), or deployable as a
899 separate element at the surface (AWL/S). The latter option requires that the arm holds the instrument and
900 deposits it on the surface. The reason for selecting one of other option could be based on the arm design
901 constrains but also on the biochemical cleanliness conditions. AWL detects large organics molecules
902 (proteins, lipids, etc.) and to avoid false positives the level of biochemical cleanliness of the arm solid
903 sampler should be stricter than if it only supplies samples to an organic analyser or a vibrational
904 spectrometer. If the AWL works at the surface it has its own sampler; if it is inside the lander it only has a
905 module to liquefy the sample. From an engineering point of view, it is more efficient to have the AWL
906 inside the lander. The AWL could also host the magnetometer with a small increase of mass (deployment
907 boom, sensor head and electronic) and if it is on the lander it could also include the thermogravimeter. In
908 this case, the ESA contribution is a totally independent package, with clear interfaces with the lander.

909 **AWL/S description:** the block diagram of the Astrobiology Wet Laboratory (AWL) is shown in Figure
910 24. In the AWL/S option it is composed of: i) a Sample Acquisition Module in charge of making a 10 cm
911 hole to take a liquid sample, ii) the Data Processing Unit which controls the instrumentation and the
912 communication with the lander; iii) a Power Unit composed by the batteries and circuit to regulate the
913 power and distribute it to the other units; iv) a Communication Unit to establish the connections with the
914 lander via an umbilical cable. An external structure support allows one to deploy the AWL with the lander
915 manipulator. For the Sample Acquisition Module (SAM), we have evaluated different alternatives for
916 drilling (Ulamec 2007, Biele 2011, Weiss 2011, Sakurai 2016), taking into account the limitations on
917 resources and trying to reduce as much as possible the use of any mechanism. The most promising option
918 is the use of a drilling system based on laser. Sakurai (2016) has demonstrated the capabilities of this
919 concept. Some of the characteristics of SAM are summarized in Table 7:

920 Figure 25 shows a sketch of the concept proposed. The water sample is taken in two steps: i) the first 5
921 cm of ice (degraded by the radiation) are sublimated by the laser and ii) the tube is moved down by a
922 pneumatic actuator and once in contact penetrates by 5 cm in the ice. The tube is pressurized and heated
923 to provide conditions in which the water is stable. At this moment the sample is sucked by a syringe
924 (controlled by a spring) to fill the sample deposit. From this deposit the instruments are filled. A single
925 pressurized deposit (nitrogen TBC) is used for tube movement and pressurization. The most critical
926 components of the AWL/S are the batteries. They are the heaviest element and need to be controlled
927 above a determined temperature to maintain their performances. For radiation protection, the Warm and
928 Shielding Box has a thickness of 18 mm Al to allow the use of space standard components. Figure 26
929 shows the AWL mechanical configuration. A warm and shielding box (WSB) is used to maintain the
930 operational temperature and protect all the electronics for radiation. The WSB will guarantee by design
931 bio-cleanliness after integration. The SAM will have an isolation lid that will be closed once at the end of
932 the integration to maintain biological cleanliness. An opening protected with an EPA filter will help the
933 decompression during launch. The external structure supports the magnetometer boom and allows
934 hanging to the lander articulated arm.

935 This configuration allows ejection from the lander if for some scientific reason it was recommended to
936 explore some site far from it. The AWL side could be equipped with small airbags following a similar
937 concept implemented in the Pathfinder lander. A set of petals could guarantee its vertical orientation.

938 **AWL/L description:** The main difference with the AWL/S is the SAM, which in this case is reduced to a
939 module to liquefy the sample and has no batteries, making the Power Unit much simpler. The process for
940 obtaining the liquid sample is similar to the one proposed for the AWL/S.

941 **4.2.3. Exploring the potential of the Square Kilometre Array for enhanced data downlink**
942 **capabilities.**

943

944 The Square Kilometre Array (SKA)¹ is an international project aiming to eventual construction of the
945 radio telescope with the collecting area of the order of one square kilometer. Its physical construction is to
946 start in 2021 in two locations, in Western Australia and South Africa, with the full operational
947 deployment well before the realistic launch date of the mission described in this paper. The SKA part
948 located in South Africa, the so-called SKA-Mid, will cover the standard deep space communications radio
949 bands at 2.3 and, importantly, 8.4 GHz, the latter being one of the main operational data downlink bands
950 for the JEM mission. The SKA1-Mid, the first implementation part of the complete SKA project, is
951 presented in detail in Annex IV.

952

953 The SKA's high sensitivity warranted by its unprecedented collecting area has been considered as an
954 important asset for potential deep space communication applications early in the SKA project
955 development stage (e.g., Bij de Vaate et al. 2004, Fridman et al. 2010). The use of SKA1-Mid for deep
956 space communication has also been considered during the detail design phase (Schutte 2016). A
957 preliminary discussion between the JEM proposing team and the SKA Organization has identified a
958 significant mutual interest in using the SKA to enhance the data downlink capability of JEM for short
959 periods during each of the three generic science sequences: (Sequence B) SKA will be able to increase the
960 data volume returned to Earth from the carrier-orbiter by about an order of magnitude; (Sequence A) SKA
961 might be able to receive data directly from the lander or from the JEM cubesat, without a relay by the
962 orbiter; (Sequence C) finally, SKA could directly receive data from the orbiter during the critical descent
963 science phase, thus solving the platform pointing conflicts between the high-gain antenna and the INMS
964 instrument. An in-depth investigation of engineering and operational issues of the SKA use as a JEM
965 science data reception station will be addressed at the appropriate phases of the JEM project. Some
966 preliminary engineering considerations are given in Annex IV. As it becomes clear from the estimates
967 presented there, SKA-Mid could increase deep space telemetry rates by more than an order of magnitude
968 for short communication sessions.

969 **5. Proposed international collaboration schemes:**

970 We propose the following share of responsibilities between ESA and NASA, to be discussed by the two
971 agencies: (1) The two baseline platforms would be operated by NASA with the support of ESA; (2)

¹ <https://www.skatelescope.org>, accessed 2020.03.23.

972 NASA would build and operate the lander platform and study with ESA the possibility of deploying from
973 that platform a small ESA-provided « Astrobiology Wet Laboratory (AWL)» as an option; (3) ESA
974 would take a major responsibility in the delivery of the carrier/orbiter/relay platform, ranging from the
975 delivery of the full platform to the delivery of an integrated « science investigation platform » and of
976 critical subsystems; (4) The proposed selection of scientific investigations on the different flight elements
977 would be validated by ESA for the carrier/orbiter and by NASA for the lander and will likely include
978 contributions from the two corresponding scientific communities. ESA would support the developments
979 required to reach TRL6 during the study phase for the AWL, the MPAS and the MPP sensors. ESA
980 would initiate early in the project the planetary protection plan and its implementation.

981 **6. Summary and conclusions**

982 In this article we described the design of an exciting planetary mission to search for bio-signatures at
983 Jupiter's ocean moon Europa and characterize it as a potential habitat. We started from a more general
984 question: what are the evolutionary properties of a habitable moon and of its host circumplanetary system
985 which make the development of life possible. By choosing the Jupiter system as our destination, we can
986 build on the advanced understanding of this system which the missions preceding JEM, Juno, JUICE and
987 Europa Clipper will provide. We propose the following **overarching goals** for the JEM mission:
988 **Understand Europa as a complex system responding to Jupiter system forcing, characterise the**
989 **habitability of its potential biosphere, and search for life at its surface and in its sub-surface and**
990 **exosphere.** These goals can be addressed by a combination of five Priority Scientific Objectives
991 providing detailed constraints on the science payloads, on the platforms that will carry them and on the
992 mission architecture.

993 Scientific observations will be made during three sequences: 1- on a high-latitude, low-latitude European
994 orbit providing a global mapping of planetary fields (magnetic and gravity) and of the neutral and charged
995 environment; 2- in-situ measurements at the surface, using a soft lander focusing on the search for bio-
996 signatures at the surface and sub-surface using analytical techniques in the solid and liquid phases, and a
997 surface geophysical station; 3- measurements of the very low exosphere in search for biomolecules
998 originating from the surface or sub-surface during the final descent phase.

999 These observations will be done by two science platforms: a soft Europa lander and an orbiter. In this
1000 concept, the carrier/orbiter will carry the lander stack from Earth to a European orbit from which it will
1001 release the lander. It will then provide the data relay during the lander operations and perform science
1002 operations during the relay phase on a halo orbit of the Europa-Jupiter system, before moving to its final
1003 European science orbit for three months.

1004 Our orbiter payload includes seven well-proven instruments to characterize planetary fields and the
1005 plasma, neutrals and dust environment. To efficiently address the radiation issue, we propose to decouple
1006 the sensor heads from the other parts of the electronics and to group these parts in a dedicated vault or a
1007 well-shielded location within the platform. Appropriate planetary protection measures corresponding to at
1008 least Planetary Protection Category IVb will be applied to all subsystems, including the payload and the
1009 spacecraft element.

1010 Our lander science platform is composed of a geophysical station and of two complementary astrobiology
1011 facilities carrying biosignature characterization experiments operating respectively in the solid and in the
1012 liquid phases. The development of the liquid phase laboratory, called AWL for “Astrobiology Wet
1013 Laboratory”, could be a specific European contribution. The two astrobiology facilities will be fed by a
1014 common articulating arm operating at the platform level that will collect the samples at the surface or sub-
1015 surface. We are proposing two alternative options for the deployment of AWL: inside the main platform,
1016 where it would benefit from all its infrastructure and services, or outside of it as an independent sub-
1017 platform, to be deployed with the help of the articulated arm.

1018 Given their investments and experience in the space exploration of the Jupiter system, NASA and ESA
1019 are in the best position to collaborate on the implementation of JEM. To make JEM an affordable and
1020 appealing joint exploration venture for the two agencies, we propose an innovative distribution of roles;
1021 ESA would design and provide the carrier-orbiter-relay platform while NASA would provide an SLS
1022 launcher, the lander stack and most of the mission operations. We showed in this article that this delivery
1023 is technically possible using a safe technical approach, taking advantage of a double heritage of European
1024 developments for space exploration: the Juice spacecraft for the JEM orbiter avionics, and an adaptation
1025 of the ORION ESM bus for its structure. Following this approach, we believe JEM will be a very
1026 appealing joint venture of NASA and ESA, working together towards one of the most exciting scientific
1027 endeavours of the 21st century: search for life beyond our own planet.

1028
1029 Acknowledgements: The authors received support from the sponsors of their home institutions during the
1030 development of their projects, particularly at the two institutes leading this effort: at IRAP, Toulouse, MB
1031 and NA acknowledge the support of CNRS, University Toulouse III – Paul Sabatier and CNES. At CAB,
1032 Madrid, OPB and JGE acknowledge the support of INTA and Spanish MINECO project ESP2014-55811-
1033 C2-1-P and ESP2017-89053-C2-1-P and the AEI project MDM-2017-0737 Unidad de Excelencia “María
1034 de Maeztu.”. We would also like to extend special thanks to the PASO of CNES for its precious
1035 assistance and expertise in the design of the mission scenario.

1036

1037 **ANNEX I: Summarized traceability matrix for JEM / OVERARCHING GOAL: Understand**
1038 **Europa as a complex system responding to Jupiter system forcing, characterize the habitability of**
1039 **its potential biosphere, and search for life at its surface.**

1040

1041 **ANNEX II: JEM orbiter system design**

1042 The main design drivers of the carrier/orbiter are:

1043 - to accommodate a 2,8 tons lander stack, to sustain the lander during cruise and to eject it with the highest
1044 accuracy and reliability,

1045 - to accommodate a very large tank capacity to provide the required delta V (~ 3 km/s) for a ~13 tons
1046 composite,

1047 - to accommodate large appendages (large solar generator to cope with low solar flux and high radiation
1048 degradation, high gain antenna, instruments boom to support the orbiter's instruments suite),

1049 - to maintain spacecraft resources and reliability in a very harsh environment (high radiation in European
1050 orbit, very cold temperature at Jupiter),

1051 - to provide a sound mechanical interface with the Space Launch System (SLS).

1052 The projected mass budget and ISP of the carrier and lander stack are shown in Table A2.1.

1053 Delta and propellant budget. The launch and transfer strategy (NASA design) features a large Deep Space
1054 Maneuver (DSM) and an Earth Gravity Assist to reach Jupiter. This so-called DVEGA scenario was also
1055 used by Juno. The SLS performance (Block 1 version) for this scenario is 13,3 tons. The delta V budget
1056 during the Jupiter Tour (Table A2.2) is taken from the JPL design known as the "12-L1" Tour ("Jovian
1057 tour design for orbiter and lander missions to Europa", Campagnola et al, 2014). The total delta V budget
1058 amounts to 3050 m/s. Assuming an orbiter dry mass of 2500 kg and a lander stack of 2800 kg, the
1059 propellant budget reaches 7900 kg. The composite wet mass (13,2 tons) is compatible with the launcher
1060 capability. The maximum dry mass requirement put on the JEM orbiter is therefore 2500 kg, including
1061 20% system margin. Note that an additional gravity assist at Earth would allow to reduce the DSM
1062 intensity, and provide very significant additional mass margin at the cost of one additional year of
1063 transfer.

1064 As an alternative to the SLS, use of a Falcon Heavy launcher would significantly reduce the mission cost,
1065 though likely at the expense of an additional Earth gravity assist: we did not study this option in detail but
1066 it should be kept in mind.

1067 The delta budget is consistent with the JPL mission profile (DV-EGA transfer, 12-L1 Jupiter Tour). The
1068 propellant budget fits within the Orion ESM capability (8600 kg) with margin. Based on these key

1069 figures, it has been possible to perform a rough study of the JEM orbiter. Figure A2.1 shows its baseline
1070 configuration, stacked and deployed.

1071 Radiation design: The radiation system design is a compromise between shielding mass and rad-hard
1072 electronics development. The radiation analysis results in a TID of 50 krad inside a 22 mm Al sphere.
1073 This 50 krad value is the design target considered for JUICE, and it is proposed to be considered also for
1074 JEM to maximize the reuse of the JUICE electronics. Assuming a compact 0,5 m³ vault (half the JUICE
1075 volume), the 22 mm equivalent Al leads to 188 kg of lead shielding (4.5 mm of lead thickness, assuming
1076 15% of shielding efficiency thanks to use of a high Z material).

1077 Power sizing: Power generation in LILT conditions (50W/m²-130°C) and under the very harsh radiation
1078 environment at Europa is a challenge. Displacement damage is produced in the solar cells under electrons
1079 and protons irradiation, significantly reducing the EOL power. To reduce cost, mass and complexity, the
1080 JUICE solar generator (85 m²) is downsized for JEM to 78 m² (4 panels of the 5-panel JUICE wings are
1081 kept). The same design approach as currently used on JUICE is proposed for JEM, with a 300 µm thick
1082 cover glass protecting the solar cells. Extrapolating the JUICE solar generator's performance on the JEM
1083 mission profile demonstrates that a 78 m² solar generator will provide around 650 W end of life. This
1084 value is used as power requirement for JEM orbiter design.

1085 Mechanical, propulsion and thermal control: The Orion ESM mechanical bus is reused and adapted for
1086 JEM. The primary structure is a cylindrical shape of 4 m in diameter and 3 m in height, made of
1087 aluminum-lithium alloy. All equipment specific to the Orion mission (e.g. life support systems) are
1088 removed from the central box to free space for the Lander Stack, that is accommodated on the top face of
1089 the orbiter (as the Orion Crew Vehicle), with the Solid Rocket Motor (SRM) fitted inside the inner
1090 rectangular cylinder. Guided rails are added within the inner box to ease and secure the lander's ejection.
1091 The mechanical interface between the orbiter and the lander is made with a skirt mounted on the SRM
1092 tank. A planetary protection back shell covers the entire lander stack to keep it clean. The lower part of
1093 the inner cylinder accommodates the 0,5 m³ lead-shielded electronics vault. The JEM bi-propellant
1094 propulsion system makes the maximum reuse of the ESM design. The 27 kN main engine is removed, and
1095 only the 4 nominal 490 N (Aerojet R-4D) are kept. These 4 main engines provide a 2 kN thrust used in
1096 the nominal case for the large Jupiter and Europa Insertion Manoeuvres (JOI, EOI). The Reaction Control
1097 System (RCS) is downgraded, replacing the 220 N engines by 22 N thrusters (MOOG DST-12, used on
1098 JUICE). 4 pods of 3 x 22 N thrusters provide attitude control during main engines boost and a safe back-
1099 up in case of one 490 N failure. Two upper pods of 4 x 22 N provide attitude control around Z. The 4
1100 large propellant tanks (with a maximum capacity of 8600 kg of propellant, compatible with JEM needs of
1101 7900 kg) and the 2 pressurant tanks are kept. The Orion ESM thermal control system (designed to reject 5
1102 kW of heat) is considerably simplified and downsized for a fully passive control system, using a network

1103 of surface heat pipes to transport the heat to the radiators. The same MLI blankets (with external
1104 conductive layer) are used as for JUICE, to ensure a clean EMC environment for the orbiter's plasma
1105 package.

1106 Power system: A two-wing 78 m² solar generator provides the required 650 W EOL power. The JUICE
1107 PCDU is reused to condition the electrical power on a regulated 28 V bus. A 167 Ah battery (JUICE
1108 battery downscaled to 3 modules) supplies the spacecraft during the 3 hours eclipses in European orbit, and
1109 complements the solar generator in high power phases such as insertion manoeuvres. The PCDU also
1110 provides the electronics of the Solar Array Drive Mechanism (SADM), to optimize radiation shielding.

1111 Avionics: The JUICE avionics is reused for the JEM orbiter. The central computer, the science mass
1112 memory and the Remote Interface Unit (RIU) are packaged into a single unit to improve shielding
1113 efficiency. Attitude control is based on a gyro-stellar estimation filter, reaction wheels for fine pointing
1114 (high gain antenna, laser altimeter) and RCS thrusters. The X-band communication system is reused from
1115 JUICE and based on a Deep Space Transponder, a 2,5m high gain antenna, and two low gain antennas for
1116 communication in LEOP and emergency TC link at Jupiter. Two UHF antennas (reused from Mars
1117 Express) are used for lander TM recovery.

1118 Relay Operations: The concept of operations is driven on one side by the configuration of the antennas
1119 and on the other side by the mission needs. The HGA (High Gain Antenna) is located below the
1120 spacecraft and the large beam width UHF antenna is located on a lateral face of the spacecraft. This
1121 ensures that there is, for any orbit around Europa and out of Jupiter eclipses, a significant section of the
1122 orbit where pointing HGA towards Earth is compatible with having UHF antenna in visibility of the
1123 lander. The HGA allows a data rate towards earth of more than 15 kbps for a mission need that is below
1124 150 Mb per day. Thus only a small fraction of the relay orbit requires pointing of HGA towards Earth.

1125 Design for payload:

1126 A 5m magnetometer boom is used to provide a clean magnetic environment to the MAG sensors. The
1127 possibility to accommodate the JUICE recurrent 10.6m MAG boom will be investigated in Phase A. All
1128 design measures taken on JUICE to ensure the best EMC cleanliness performances are reused for JEM:
1129 the electronics vault provides an efficient Faraday cage to contain E-field radiation from electronics, a
1130 distributed single grounding point is implemented within the PCDU to avoid common mode perturbation,
1131 external surfaces (solar generator, MLI) are covered with an outer conductive coating to avoid charging, a
1132 magnetic shield is implemented on the most perturbing units (reaction wheels, motor drives). Two
1133 monitoring cameras will provide pictures of the lander's ejection. The overall resources allocation for the
1134 JEM orbiter is 50 kg and 100 W. The launch mass budget fits within the SLS capability and includes a
1135 20% system margin on the carrier's dry mass.

1136

1137
1138
1139
1140
1141
1142
1143
1144
1145
1146●
1147●
1148●
1149●
1150
1151
1152
1153
1154
1155
1156
1157
1158
1159
1160
1161
1162
1163
1164
1165
1166
1167
1168
1169
1170

ANNEX III: Orbitography for the JEM mission

Once the Carrier has released the Lander, it must act as a relay for the total duration of the Lander mission. Choosing a halo orbit around the Jupiter-Europa L1 Lagrangian point (JEL1) provides a great coverage of the landing site. The unstable nature of those orbits allows low-energy transfers, while the cost of orbit maintenance is very low.

Halo orbits are families of unstable periodic orbits in the 3-body problem around collinear Lagrangian points [*Dynamical Systems, the Three-Body Problem and Space Mission Design (Koon et al., 2006)*]. The choice of a specific halo orbit among its family is subject to a few constraints:

- The position of the landing site
- The science expected to be accomplished
- The ΔV needed to reach and to leave this orbit
- The time of flight to reach and to leave this orbit.

The variation of the radiation dose is negligible regarding the choice of a specific halo orbit.

Because of the symmetry of the 3-body problem, the landing site is assumed to be on the northern hemisphere of Europa, and the halo orbits are chosen in the southern class for this study. The results would be the same with a landing site on the southern hemisphere and with northern halo orbits. In order to investigate the Europa-magnetosphere interaction, a halo orbit near Europa is preferred.

Once a specific halo orbit is chosen, the transfer from this halo orbit to a low-altitude, near polar, circular orbit around Europa (LEO) is studied. The characteristics selected for this orbit are an inclination between 80° and 90° , and an altitude between 100m and 200km [*Europa Study 2012 (NASA)*]. First, at each position on the halo orbit, a small burn (few m/s) in the unstable direction toward Europa is performed.

Then, when one of those trajectories features an extremum of distance to Europa, the osculating orbital elements are calculated to see if they match the requirement of the LEO. A tangent burn to circularize around Europa is then applied. A set of halo orbits [*Global search for planar and three-dimensional periodic orbits near (Russell, 2006)*] labelled with ID's (Figure A3.1 and Table A3.1) was investigated in order to highlight the range of possibilities for a transfer from a halo orbit to a LEO. Figure A3.4 shows a subset of these couples of halo and transfer orbits.

The results (Figures A3.2 and A3.3) indicate a ΔV between 440m/s and 540 m/s, for a duration of 1-7 days. Some halo orbits have more possibilities of transfer than others. Some of them don't have any possibilities of transfer (ID = 275). The closer to Europa the halo orbit is, the higher the ΔV is. If we take a look at the range of possibilities of LEO's for each halo orbit, choosing a more specific LEO could limit the possibilities even more. Characteristics of some of the reachable LEO orbits are shown in Table A3.2, and characteristics of the corresponding transfer orbits in Table A3.3.

1171 If a specific LEO is necessary, one solution would be to pick the transfer to a LEO close to the desired
1172 LEO, and then perform a change of altitude and a change of inclination. A change of altitude from 200km
1173 to 100km is 40m/s while a change of inclination of 10° is 240m/s (which is not negligible). However, we
1174 can expand the possibilities of transfer using a non-negligible burn to leave the halo orbit. To limit the
1175 degree of freedom of this problem, a simple tangent burn is used [*Connecting halo orbits to science orbit*
1176 *at planetary moons (Bokelmann and Russell, 2017)*].

1177 The number of possibilities is largely expanded. Even if the ΔV tends to be higher, a transfer with less
1178 than 530 m/s and a reasonable time of flight can always be found (less than 3 days). Even more, the
1179 spectrum of reachable LEO is also wide. The last thing to be done is to select the transfer best suited for
1180 the mission.

1181
1182

1183 **ANNEX IV: Square Kilometre Array as a data downlink reception station for JEM**

1184 This annex gives a preliminary overview of the potential capabilities of the advanced radio astronomy
1185 facility, the Square Kilometre Array (SKA), and in particular its first implementation phase for medium-
1186 range frequencies, SKA1-Mid as an Earth-based receiving station for the JEM science data downlink.
1187 The primary mission of SKA is the advancement of radio astronomy. However, exploratory discussions
1188 on a potential use of some fraction of the SKA observing time enhancing science output of planetary
1189 missions are underway too. Basic parameters of the SKA1-mid used in the estimates presented below
1190 are taken from the SKA Info Sheets² and references therein.

1191

1192 **A4.1 Description of SKA1-Mid**

1193

1194 The SKA1-Mid instrument will be an array of 197 offset Gregorian dishes and associated signal
1195 processing equipment (figure 4.1). The dishes will provide a total collecting area of 32,700 m². Of these,
1196 64 dishes have been constructed as part of the MeerKAT precursor telescope, while an additional 133
1197 dishes will be constructed for SKA1. MeerKAT is already operational and early scientific results
1198 include the discovery of more than 1200 new galaxies in its First Light image³ and the highest
1199 resolution images yet of our galactic center⁴.

² <https://www.skatelescope.org/technical/info-sheets/>, accessed 2020.03.23.

³ <https://www.sarao.ac.za/media-releases/meerkat-joins-the-ranks-of-the-worlds-great-scientific-instruments-through-its-first-light-image/>, accessed 2020.03.25.

⁴ <https://www.sarao.ac.za/south-africas-meerkat-discovers-giant-radio-bubbles-at-centre-of-milky-way/>, accessed 2020.03.25.

1200 SKA1-Mid will re-use much of the existing MeerKAT infrastructure, including the shielded
1201 subterranean Karoo Array Processor Building and the electrical power system. SKA1-Mid is being
1202 designed for 24/7 operation and an overall time efficiency greater than 0.9. Several critical systems
1203 (power supply, core power distribution, processor cooling, etc.) are redundant. The full SKA1-mid array
1204 will consist of a circular dense core and three spiral arms extending to a distance of approximately 90
1205 km from the core (figure 4.2). The instrument will be located near Carnarvon in the Karoo region of
1206 South Africa, approximately centered on the following coordinates: 30°42'46.37"S, 21°26'35.50"E.

1207 SKA1-Mid will cover the frequency range 0.35–13.8 GHz in 5 bands. The cryogenically cooled Band 5
1208 receivers of SKA1-mid will cover the frequency range from 4.6 to 13.8 GHz, and will therefore include
1209 the X-band telemetry allocation around 8.4 GHz.

1210 The SKA1-Mid construction roll-out will progress through several array releases, with all dishes (and
1211 MeerKAT) integrated and commissioned by 2027. It is likely that a series of expansions and upgrades
1212 will be implemented following 2027, as part of the future SKA2 project.

1213

1214 **A4.2 Summary of SKA1-Mid potential for the support to deep space missions**

1215

1216 The sensitivity of SKA1-Mid in terms of the ratio G/T (where G is the telescope gain and T is the
1217 system noise temperature) will be about 25 times that of a generic modern X-band 35 m Earth-based
1218 deep space data reception station. This leads to three transformational capabilities for deep space
1219 missions. In particular,

1220 • SKA1-mid will be able to increase the data rate of science data downlink delivered to Earth
1221 comparing to the currently operational deep space communication assets.

1222 • SKA1-mid will be able to receive data directly from small descent and landing probes or from a
1223 mini-satellites (e.g., a JEM cubesat), without a relay spacecraft.

1224 • SKA1-mid could directly receive data from a mission spacecraft during critical phases of high
1225 scientific interest, like a descent to a planetary surface, radio occultation, etc.

1226 In many cases, the SKA1-mid facility will be the only instrument on Earth capable of providing these
1227 capabilities, and could therefore be an important resource for future deep space exploration.

1228 In order to evaluate the capacity of SKA1-mid for data reception, a model link budget has been
1229 analyzed under the following assumptions:

1230 • Spacecraft transmitter Power: 50 W

1231 • Onboard HGA gain: 44.8 dB

1232 • Pointing loss: 0.1 dB

1233 In the X-band, the SKA1-mid Band 5 receiver figure of merit (G/T) has been conservatively estimated
1234 as 67.22 dB. Assuming the following link parameters:

1235

- 1236 • Link margin: 3 dB;
- 1237 • Bit error rate (BER): 10^{-5} ;
- 1238 • Ratio of the energy per transmitted bit, E_b , to the spectral noise density, N_0 ,
1239 $E_b/N_0 = 0.3$;
- 1240 • Modulation: QPSK;
- 1241 • Forward error correction: turbo code with the code rate 0.25;
- 1242 • The distance between the spacecraft and Earth: 8×10^8 km.

1243 These parameters result in the over-the-air data rate of 1.6 Mbps when using SKA1-mid as reception
1244 station, and up to 2.3 Mbps under ideal conditions. This calculation should be considered an initial
1245 estimation, and further study is required. The major underlying assumption is that 60% of the collecting
1246 area of the SKA1-mid array can be used for reception, due to the difficulty in correcting phase errors of
1247 the outer spiral arm dishes. Thus, a conservative working assumption is that dishes up to a radius of
1248 approximately 1.3 km (i.e. most of the core) can be successfully phased up.

1249 For radio telescopes it is customary to express their instantaneous sensitivity performance in terms of
1250 effective collecting area over system temperature (A_e/T_{sys}). This parameter for SKA1-mid at 8.4 GHz is
1251 $A_e/T_{sys} = 890 \text{ m}^2/\text{K}$. At a radius of 1.3 km, the total available sensitivity is reduced to 60% of the total,
1252 giving $A_e/T_{sys} = 534 \text{ m}^2/\text{K}$.

1253

1254

1255 **BIBLIOGRAPHY**

- 1256 Baross, J.A. and S. E. Hoffman (1985). *Origins of Life and Evolution of the Biosphere* 15(4): 327-345.
- 1257 Bills, B., Ray, R. (2000). *J. Geophys. Res.*, 105 (E12), p. 29277-29282
- 1258 Biele J. et al. (2011). *Adv. Space Res.*48, 755-763
- 1259 Bij de Vaate J.G. et al. (2004), '*Spacecraft Tracking Applications of the Square Kilometre Array*', 3rd
1260 International Workshop on Tracking, Telemetry and Command Systems for Space Applications, TTC
1261 2004, 93–100 (<https://arxiv.org/abs/2002.10024>)
- 1262 Bird M.K., Allison M., Asmar S.W., Atkinson D.H., Avruch I.M., Dutta-Roy R., Dzierma Y., Edenhofer
1263 P., Folkner W.M., Gurvits L.I., Johnston D.V., Plettemeier D., Pogrebenko S.V., Preston R.A., Tyler
1264 G.L., 2005, *Nature* 438, 800-802
- 1265 Blöcker A., J. Saur, and L. Roth (2016), *J. Geophys. Res.*., 121, doi: 10.1002/ 2016JA022479.
- 1266 Bocanegra Bahamón T.M., Molera Calvès G., Gurvits L.I., Duev D.A., Pogrebenko S.V., Cimò G., Dirx
1267 D., and Rosenblatt P., 2018, *AA* 609, A59
- 1268 Bocanegra Bahamón T.M., Molera Calvès G., Gurvits L.I., Cimò G., Dirx D., Duev D.A., Pogrebenko
1269 S.V., Rosenblatt P., Limaye S., Cui L., Li P., Kondo T., Sekido M, Mikhailov A.G., Kharinov M.A.,
1270 Ipatov A.V., Wang W., Zheng W., Ma M., Lovell J.E.J., and McCallum J.N. 2019, *A&A*, 624, A59
- 1271 Bokelmann, K.A., Russell, R.P.: Halo orbit to science orbit captures at planetary moons. *Acta Astron.*
1272 **134**, 141–151 (2017). <https://doi.org/10.1016/j.actaastro.2017.01.035>
- 1273 Brown M.E. and Hand K.P. (2013). *Astronomical J.* 145, 110
- 1274 Campagnola,S., Buffington,B. B., Petropoulos, A.E. (2014). *Acta Astronautica*, 100, 68-81
- 1275 Carlson R.W. et al. (1999). *Science* 286, 97-99
- 1276 Carlson et al., (2005). *Icarus* 177, 461-471
- 1277 Cassen, P., et al. (1979). *Geophys. Res. Lett.* 6(9): 731-734.
- 1278 Chazallon et al. (2004)

- 1279 Chen, E. M. A. et al. (2014). *Icarus*, Volume 229, p. 11-30
- 1280 Cooper, J. F., et al. (2009). *Planet Space Sci.*, Volume 57, Issue 13, p. 1607-1620
- 1281 Cooper J.F. et al. (2001). *Icarus* 149, 133-159
- 1282 Coustenis et al. (2019). The COSPAR Panel on Planetary Protection Role, Structure and Activities. *Space*
1283 *Research Today* 205, 14-26
- 1284 Dalton et al., (2005). *Icarus* 177, 472-490
- 1285 Dalton, J. B. et al. (2010). EGU General Assembly Conference Abstracts.
- 1286 Dirx D., Gurvits L.I., Lainey V., Lari G., Milani A., Cimò G., Bocanegra-Bahamon T.M., Visser
1287 P.N.A.M., 2017, *PSS* 147, 14–27
- 1288 Dirx D., Lainey V., Gurvits L.I., Visser P.N.A.M. 2016, *PSS* 134, 82-95
- 1289 Dirx D., Prochazka I., Bauer S., Visser P.N.A.M., Noomen R., Gurvits L.I., Vermeersen L.L.A. 2018,
1290 *Journal of Geodesy*, p. 1-16
- 1291 Duev D.A., Molera Calvés G., Pogrebenko S.V., Gurvits L.I., Cimò G., Bocanegra Bahamon T.M., 2012,
1292 *A&A* 541, A43
- 1293 Duev D.A., Pogrebenko S.V., Cimò G., Molera Calvés G., Bocanegra Bahamón T.M., Gurvits L.I.,
1294 Kettenis M.M., Kania J., Tudose V., Rosenblatt P., Marty J.-C., Lainey V., de Vicente P., Quick J.,
1295 Nicola M., Neidhardt A., Kronschnabl G., Ploetz G., Haas R., Lindquist M., Orlatti A., Ipatov A.V.,
1296 Kharinov M.A., Mikhailov A.G., Lovell J.E.J., McCallum J.N., Stevens J., Gulyaev S.A., Natush T.,
1297 Weston S., Wang W.H., Xia B., Yang W.J., Hao L.F., Kallunki J., and Witasse O. 2016, *A&A* 593, A34
- 1298 Fridman P.A., Gurvits L.I., Pogrebenko S.V. (2010) *The SKA as a Direct-to-Earth Data Acquisition*
1299 *Facility for Deep Space Science Missions*, in *Wide Field Science and Technology for the Square*
1300 *Kilometre Array*, eds. S.A. Torchinsky, A. van Ardenne, T. van den Brink, A.J.J. van Es, A.J. Faulkner,
1301 ISBN 978-90-805434-5-4, p. 43-50 [PoS(SKADS 2009)006]
- 1302 Gaudin, D., ISAE master study report, 2016.
- 1303 Hand K.P. et al. (2007). *Astrobiology* 7, 1006-1022

- 1304 Hand K. P. and Chyba, C.F. (2007) Empirical constraints on the salinity of the european ocean and
1305 implications for a thin ice shell, *Icarus* 189, 424–438.
- 1306 Hand K. et al. (2017) Europa Lander Science Definition Team Report.
- 1307 Hanley, J., et al. (2014). *J. Geophys. Res.-Planets* 119(11): 2370-2377.
- 1308 Hussmann, H., Spohn, T. (2004). *Icarus*, 171, 391-410
- 1309 Hussmann, H., et al. (2010). *Space Sci. Rev.* 153 (1-4): 317-348.
- 1310 Jia, X., Kivelson, M. G., Khurana, K. , Kurth W. S. (2018), Evidence of a plume on Europa from Galileo
1311 magnetic and plasma wave signatures, *Nature Astronomy*, 2, 459-464.
- 1312 Jimenez-Jorquera C. et al., (2010). *Sensors* 10.
- 1313 Kattenhorn S.A. Prockter L.M. (2014). *Nature Geoscience* 7, 762-767
- 1314 Khurana, K.K., Kivelson M.G., Hand K.P. and Russell, C.T., Electromagnetic induction from Europa’s
1315 ocean and deep interior, in *Europa*, Arizona University Press, 571-586 (2009).
- 1316 Khurana, K. K.; Jia, X.; Kivelson, M. G.; Nimmo, F.; Schubert, G.; Russell, C. T., Evidence of a Global
1317 magma Ocean in Io’s Interior, *Science*, **332**, 1186 (2011).
- 1318 Kiefer et al. (2006). *Science* 314, 1764-1766
- 1319 Koon et al. (2006)
- 1320 Kounaves, S.P. et al., (2003). *J. Geophys. Res.* 108, 10.1029/2002JE001978
- 1321 Lainey, V., et al. (2006). *Astronomy & Astrophysics*, 456, 783-788.
- 1322 Lammer et al. (2009). *Astros. Astrophys. Rev.* 17: 181-249
- 1323 Lebreton J.-P., Witasse O., Sollazzo C., Blancquaert T., Couzin P., Schipper A.-M., Jones J.B., Matson
1324 D.L., Gurvits L.I., Atkinson D.H., Kazeminejad B., Pérez-Ayúcar M. 2005, *Nature* 438, 758-764
- 1325 Loeffler and Baragiola, (2005). *Geophys. Res. Lett.* 32, L17202
- 1326 Lunine and Shevchenko (1985)
- 1327 McCord et al., (1999). *J. Geophys. Res.-Planets* 104, 11827-11851

- 1328 McCord, T. B., et al. (2001). *J. Geophys. Res.-Planets* 106(E2): 3311-3319.
- 1329 Maize, Europa Lander SDT report to OPAG (2019)
- 1330 Mark D. et al., (2010). “Microfluidic lab-on-a-chip platforms: requirements, characteristics and
1331 applications.” *Chemical Society Reviews* 39.
- 1332 Moore, W., (2003). *J. Geophys. Res.*, 108, Issue E8, pp. 15-1
- 1333 Nimmo, F., et al. (2002). *Geophys. Res. Lett.* 29(7).
- 1334 NRC (Natl. Acad. Sci. Washington, DC). Task Group on the Forward Contamination of Europa, Space
1335 Studies Board, National Research Council (U.S.) (2000) Preventing the Forward Contamination of
1336 Europa
- 1337 Ojakangas, G.W., Stevenson D.J., (1986). *Icarus*, 66, 341-358
- 1338 Paganini, L., Villanueva, G. L., Roth, L., Mandell, A. M., Hurford, T., Retherford, K. D., Mumma, M. J.
1339 (2019) A measurement of water vapour amid a largely quiescent environment on Europa, *Nature*
1340 *Astronomy* 2397-3366, doi.org/10.1038/s41550-019-0933-6
- 1341 Pappalardo R.T., W. B. McKinnon and K. K. Khurana, *Europa*, University of Arizona Press, Tucson,
1342 (2009).
- 1343 Parro V. et al., (2005). *Planet. Space Sci.* 53, 729-737
- 1344 Parro, V. et al., (2008). *Astrobiology* 8, 987-999
- 1345 Parro, V. et al., (2011). *Astrobiology* 11, 969-996
- 1346 Patterson G.W. et al. (2012). *Icarus*, 220, 286-290
- 1347 Porco C.C. et al (2006). *Science*, 311, 1393-1401
- 1348 Pogrebenko S.V., Gurvits L.I., Campbell R.M., Avruch I.M., Lebreton J.P., van't Klooster C.G.M., 2004,
1349 in *Planetary Probe Atmospheric Entry and Descent Trajectory Analysis and Science*, A. Wilson (ed.),
1350 ESA SP-544, 197-204
- 1351 Roth L. et al. (2014). *Science* 343, 171-174

- 1352 Russell, M. J. and A. J. Hall (1997). *J. Geol. Soc.* 154: 377-402.
- 1353 Russell, M. J., et al. (2014). *Astrobiology* 14, 308-343.
- 1354 Russell, R.P. (2006) Global search for planar and three-dimensional periodic orbits near europa. *J. Astron.*
1355 *Sci.* **54**, 199–226. <https://doi.org/10.1007/BF03256483>
- 1356 Sakurai T. et al., (2016). *Cold Regions Science and technology* 121.
- 1357 Schilling, N., et al. (2004). *J. Geophys. Res.-Planets* 109(E5).
- 1358 Schmidt J. et al. (2008). *Nature* 451, 685-688
- 1359 Schutte, A.N., 2016, ‘The Square Kilometre Array Radio Telescope: Transformational Capabilities for
1360 Deep Space Missions’, 15th Reinventing Space Conference, 27 October 2016, London
- 1361 Shematovich V.I. et al. (2005). *Icarus* 173, 480-498
- 1362 Sims et al. (2005)
- 1363 Sims M.R. et al., (2012). *Planet. Space Sci.*72.
- 1364 Tobie, G., et al. (2003). *J. Geophys. Res.-Planets* 108(E11).
- 1365 Tobie, G., et al (2005). *Icarus*, Volume 177, Issue 2, p. 534-549
- 1366 Truscott, P. et al. (2011). *IEEE TRANS. NUCL. Sci.*, 58(6), 2776 – 2784.
- 1367 Tyler R., (2008). *Nature*, 456, 770-772
- 1368 Ulamec S. et al., (2007). *Rev. Environ Sci. Biotechnol.* 6
- 1369 Weiss P. et al. (2011). *Adv. Space Res.* 48
- 1370 Westall, F, Brack, A. (2018) The Importance of Water for Life, *Space Science Reviews* 214(2). DOI:
1371 10.1007/s11214-018-0476-7
- 1372 Wisdom J., (2004). *Astronom. J.* 128, 484–491.

- 1373 Witasse, O., Altobelli, N., Barabash, S., Bruzzone, L., Dougherty, M., Erd, C., Fletcher, L., Gladstone, R.,
1374 Grasset, O., Gurvits, L., Hartogh, P., Hussmann, H., Iess, L., Langevin, Y., Palumbo, P., Piccioni, G.,
1375 Sarri, G., Titov, D., and Wahlund, J.E. 2015, JUICE: A European Mission to Jupiter and its Icy Moons, in
1376 European Planetary Science Congress, pp. EPSC2015-564.
- 1377 Zahnle K. et al. (2008). *Icarus* 194, 660-674

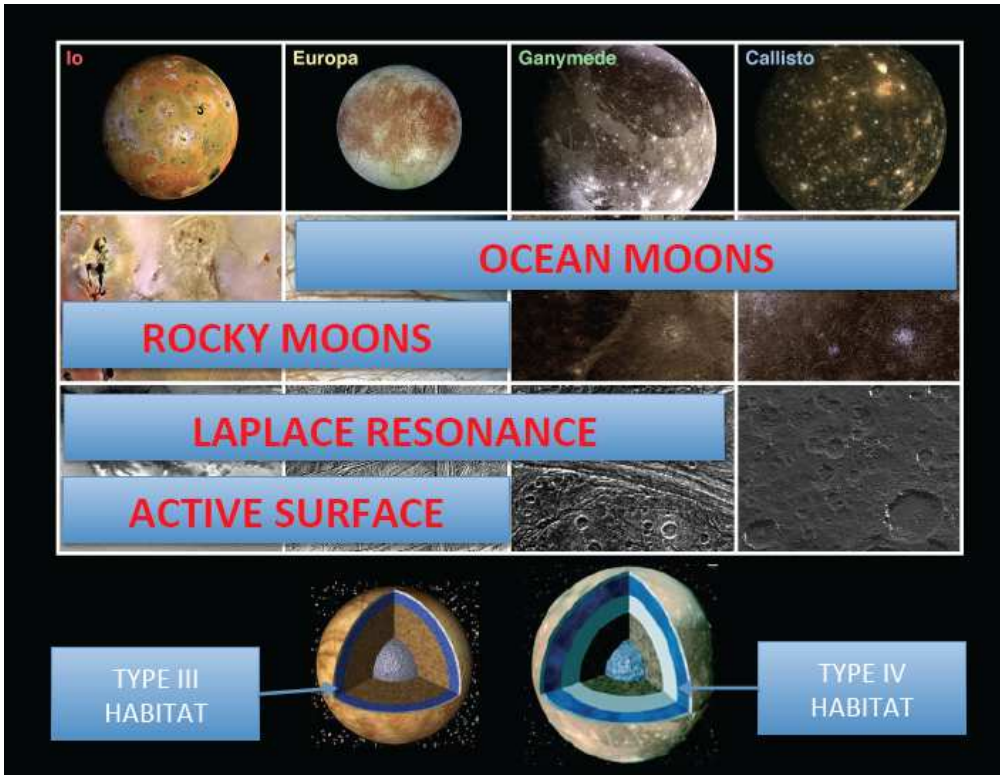


Figure 1: when the four Galilean moons are broadly characterized by the four properties shown, Europa stands out as the best possible candidate "habitable moon" (see text)

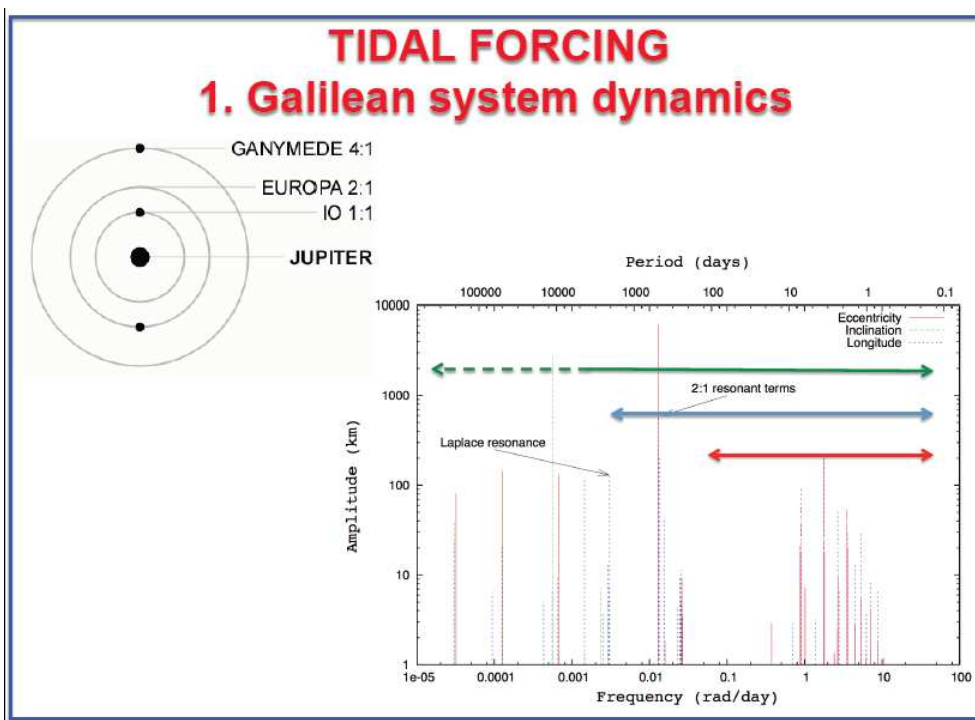


Figure 2: Tidal coupling of Europa to the Jupiter System is controlled by the dynamics of the Galilean system and its Laplace resonance (left). The figure shows the very broad spectrum of gravitational perturbations exerted on Europa's motion in its reference frame. The short periods, to the right, correspond to the orbital motions of the different satellites and their beats, which induce the most important tidal stresses. The long periods to the left correspond to all long-period oscillations of the system, and include the pendular motions in the Laplace resonance. The ranges of periods accessible respectively to JEM alone (red line), to the succession of missions to Jupiter (blue) and to the combinations of long series of astrometric measurements from the ground and from space (green) are also indicated (derived from Layné et al., 2006)

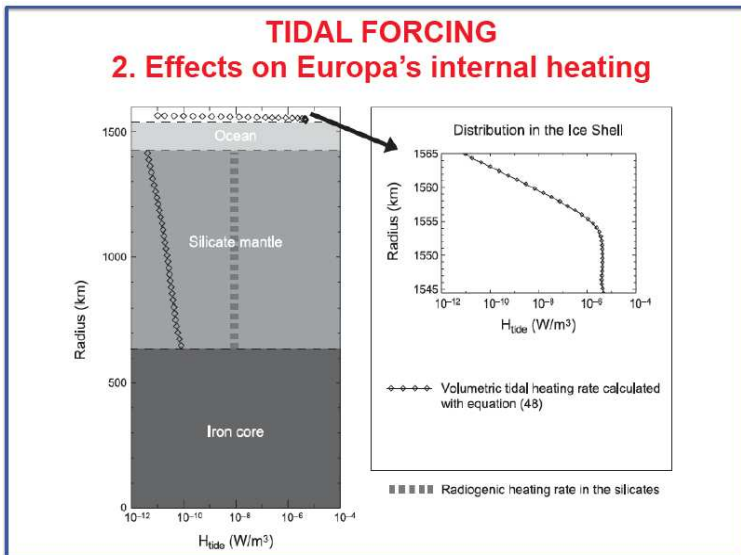


Figure 3: Tidal coupling between Io, Europa, Ganymede and Jupiter is responsible for a continuous transfer of angular momentum and energy between Jupiter and the three moons resulting in continuous heating of their interiors, ice shells, and oceans. The model of Tobie et al. (2003) shown here predicts that most of this heating goes to the ice shell in the case of Europa. Observations from an orbiter will be critical to solve this open question.

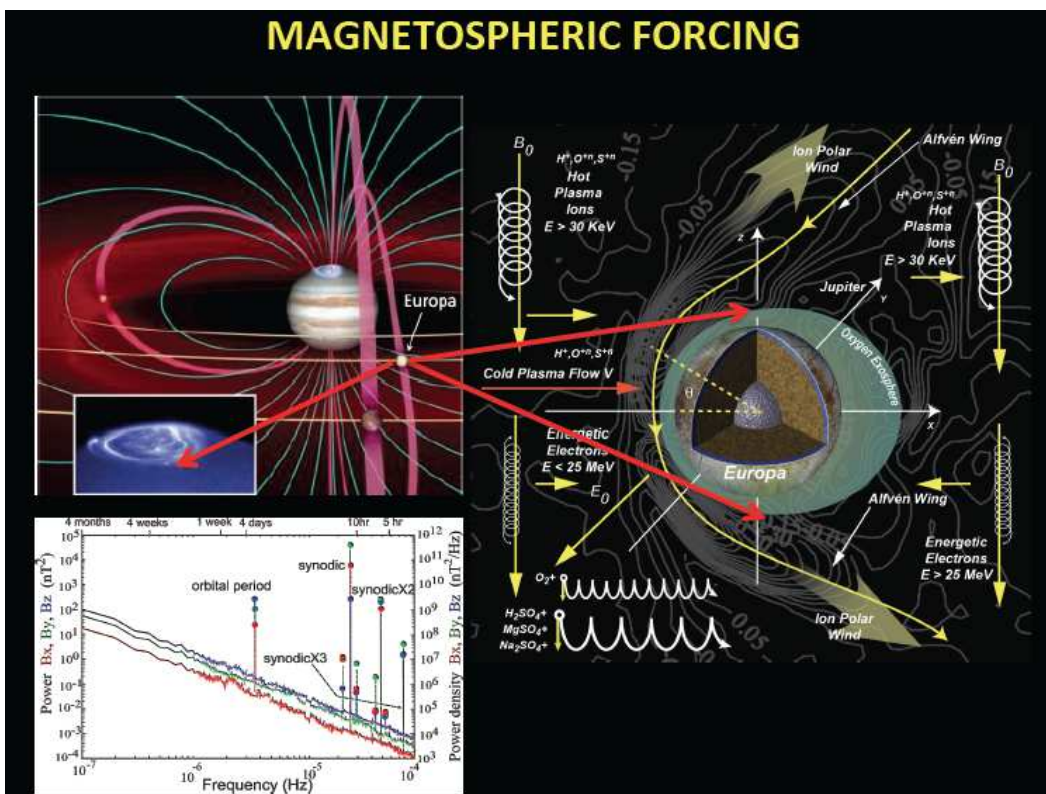


Figure 4: A simplified representation of Europa's interaction with the Jovian magnetosphere, which involves two obstacles: Europa's surface, and its subsurface ocean. This interaction generates effects from the planetary scale (a giant electrical current system coupling Europa's ionosphere to the Jovian ionosphere) to the very local European scales (the space weathering of Europa's icy surface by magnetospheric thermal and radiation belt particles). The broad-band spectrum of magnetic fluctuations associated with this interaction, seen in the European frame, allows an accurate magnetic sounding of Europa's ocean (diagram in white insert, courtesy K. Khurana).

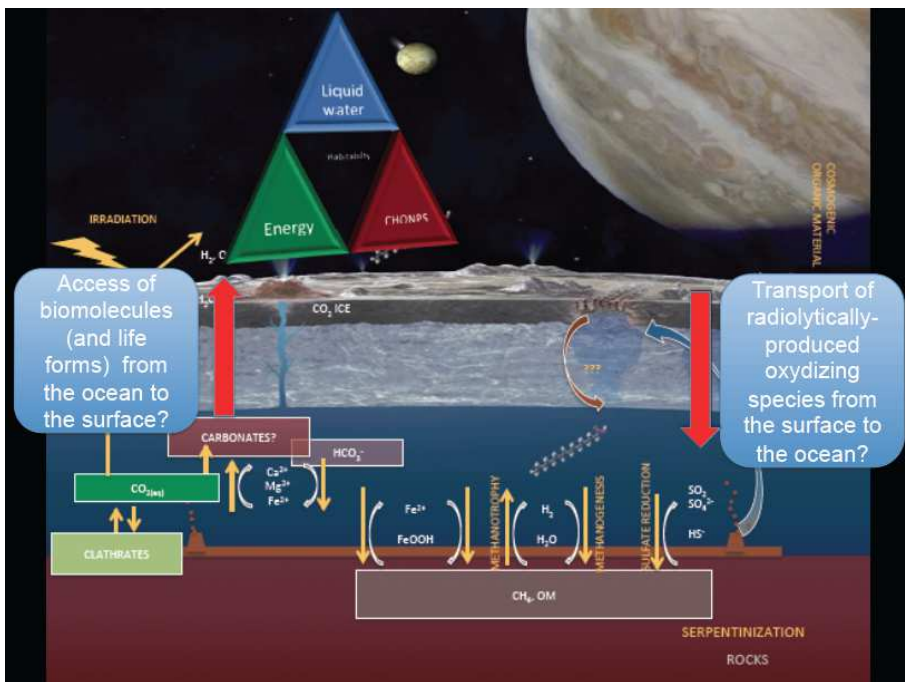


Figure 5: An examination of the properties of the layers of Europa extending from the silicate sea-floor to the ice shell surface and near-surface exosphere in the light of the "triangle of habitability" leads to the important conclusion that this aqueous internal region of Europa may be considered as a potential "dark biosphere" (see text).

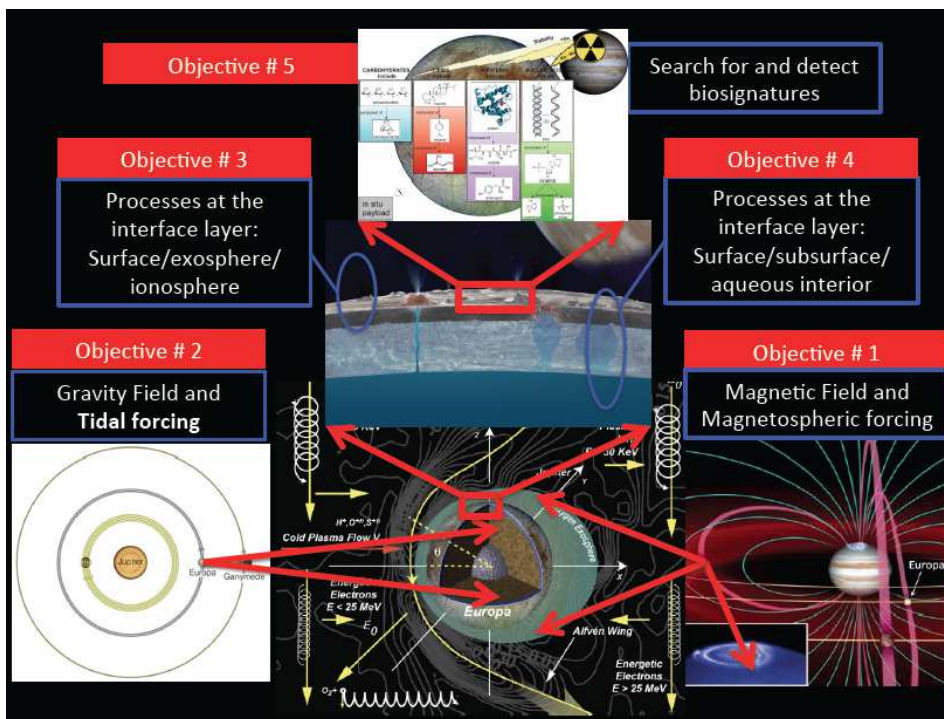


Figure 6: This logical chart of our Science Plan shows the three successive scales investigated by JEM, from bottom upwards: (1) the global Europa, a complex system responding to the two main types of Jovian forcing;

(2) the scale of Europa's potential biosphere (median figure) and (3) finally the local scale at which we will perform life detection experiments.

The JEM science plan successively articulates five "Priority Science Objectives", culminating with PSO #5, the search for biosignatures of life at the surface, sub-surface and eventually in the exosphere, to reach its Overarching Goals.

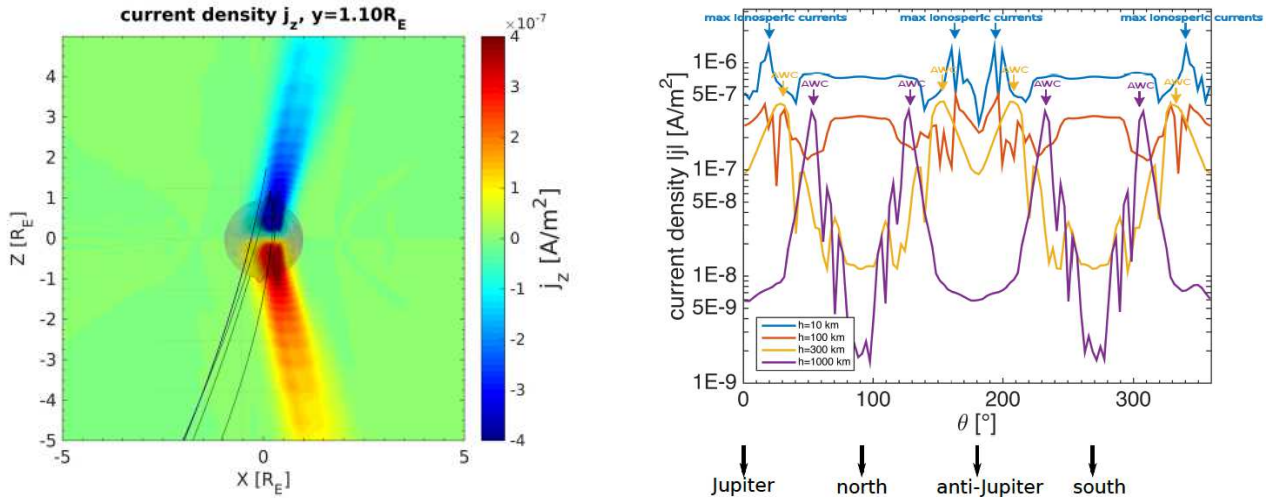


Figure 7: Ionospheric current density (left) in the XZ plane; Ionospheric current density and Alfvén wave currents (AWC) in the northern and southern hemispheres towards and away from Jupiter plotted for various altitudes along circular polar orbits. Adapted from Blöcker et al. (2016).

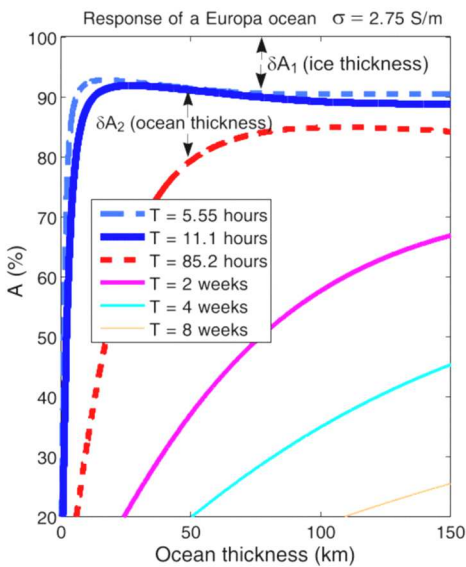


Figure 8: Response (surface induced field at pole/inducing field) of a Europa ocean with conductivity similar to that of the Earth's at six different periods. An ice thickness of 30 km was assumed for results shown in both of these figures. Figure adapted from Khurana et al. (2009)

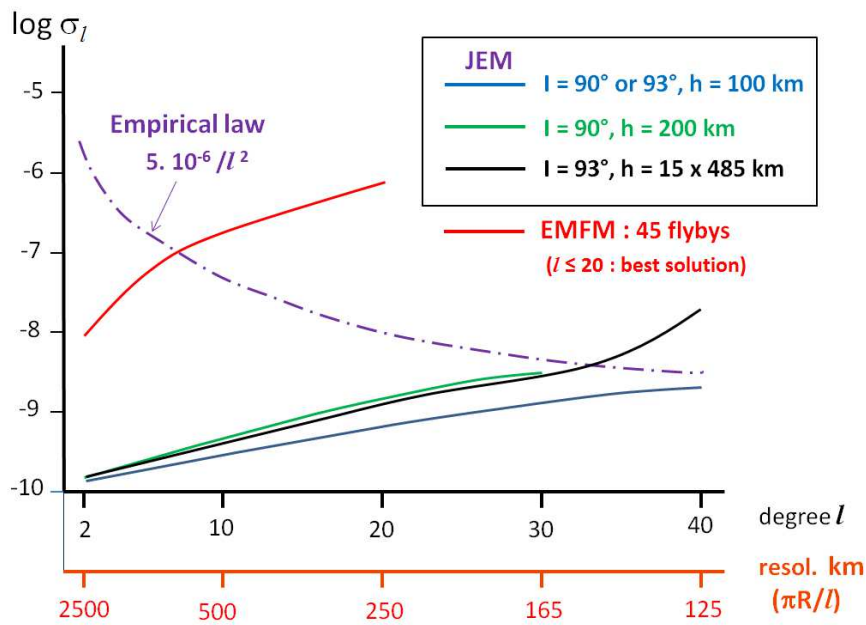


Figure 9: Determination of Europa's gravity field from two possible mission scenarios. σ_l (dimensionless) measures the uncertainty in all harmonic coefficients of degree l , corresponding to the resolution shown on the second abscissa scale. An empirical law (same shape as for other terrestrial bodies) is shown for comparison.

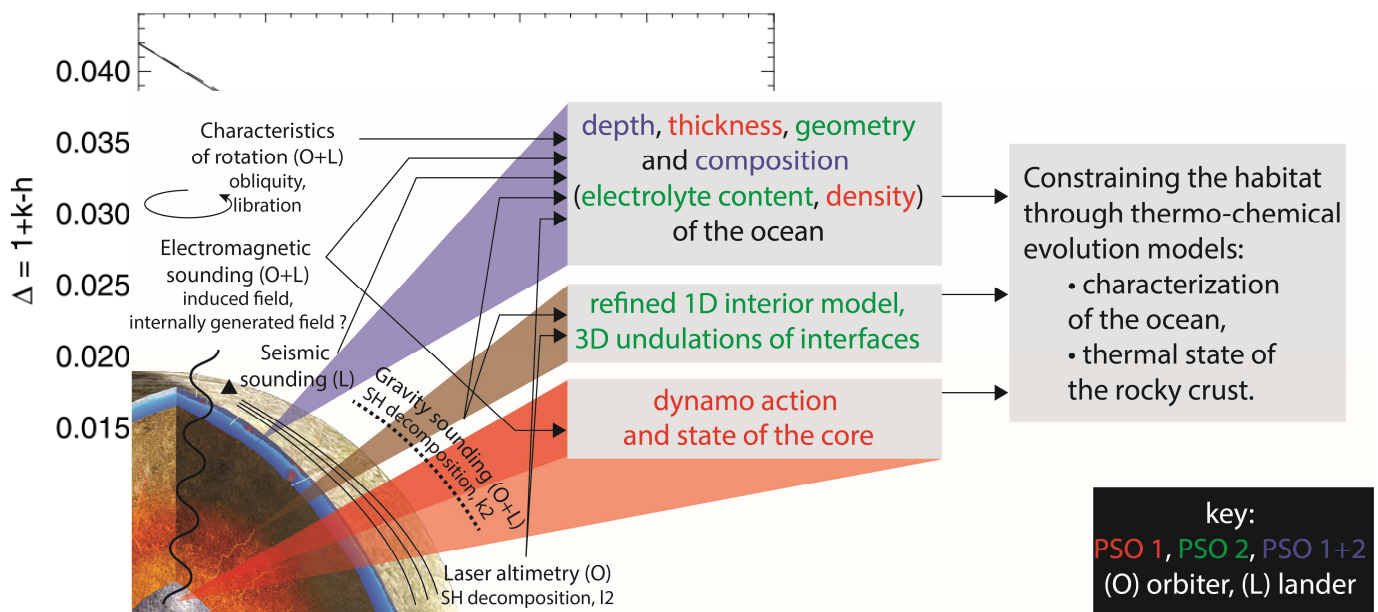


Figure 10: Synergetic orbiter / lander investigation of Europa's response to Jupiter's magnetic and gravitational forcing

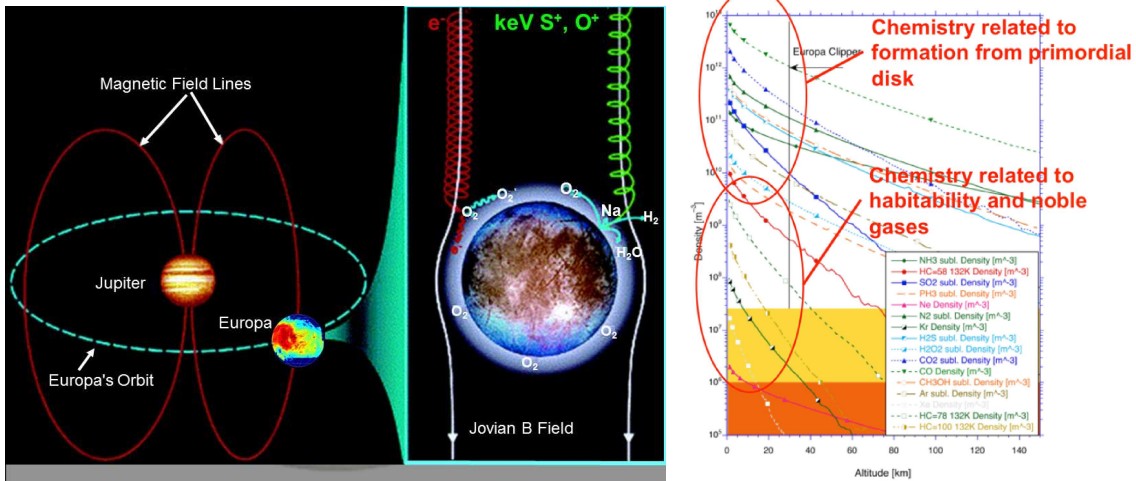


Figure 11: Cartoon of European interaction with Jupiter's magnetosphere showing how the Jovian plasma moving with Jupiter magnetospheric lines induces a trailing/leading asymmetry in the interaction. Neutral species produced by sputtering of Europa's icy surface form Europa's exosphere, which is composed essentially of O₂ and of trace species (left); calculated exospheric density profiles calculated by Shematovich et al. (2005) for species expected to be present based on the formation model (right). "SP" stands for sputtering, and "subl." stands for « released together with sublimation » water. HC are hydrocarbon molecules with the indicated mass

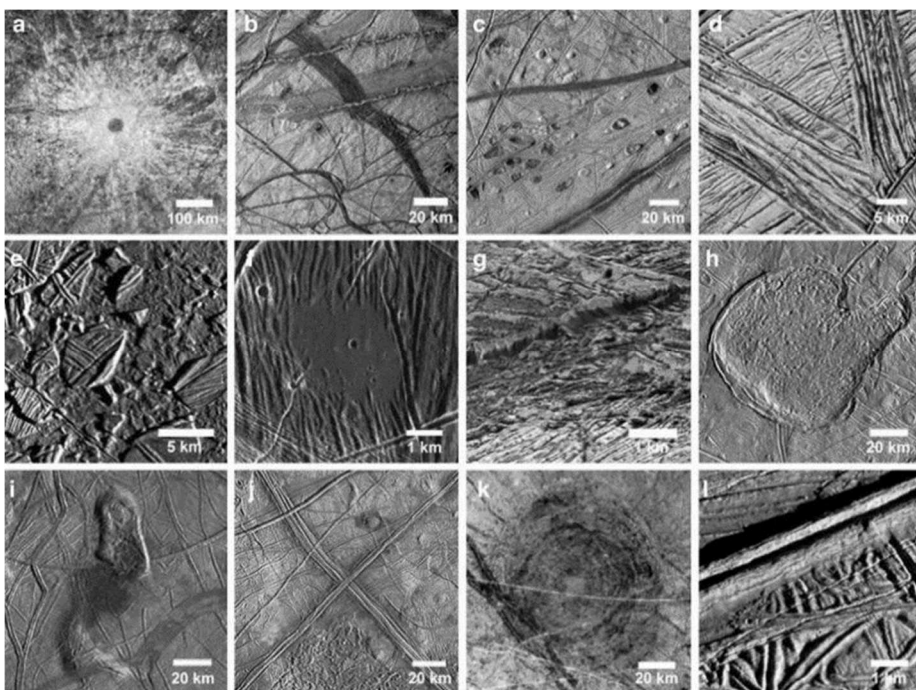


Figure 12: Variety of surface features on Europa: (a) the impact crater Pwyll; (b) pull-apart bands; (c) lenticulae; (d) ridge complexes at high resolution; (e) Conamara Chaos; (f) dark plains material in a

topographic low; (g) very high-resolution image of a cliff, showing evidence of mass wasting; (h) Murias Chaos, a cryovolcanic feature; (i) the Castalia Macula region; (j) double 7 complex ridges; (k) Tyre impact feature; and (l) one of Europa's ubiquitous ridges. (Credit: NASA/JPL/Caltech).

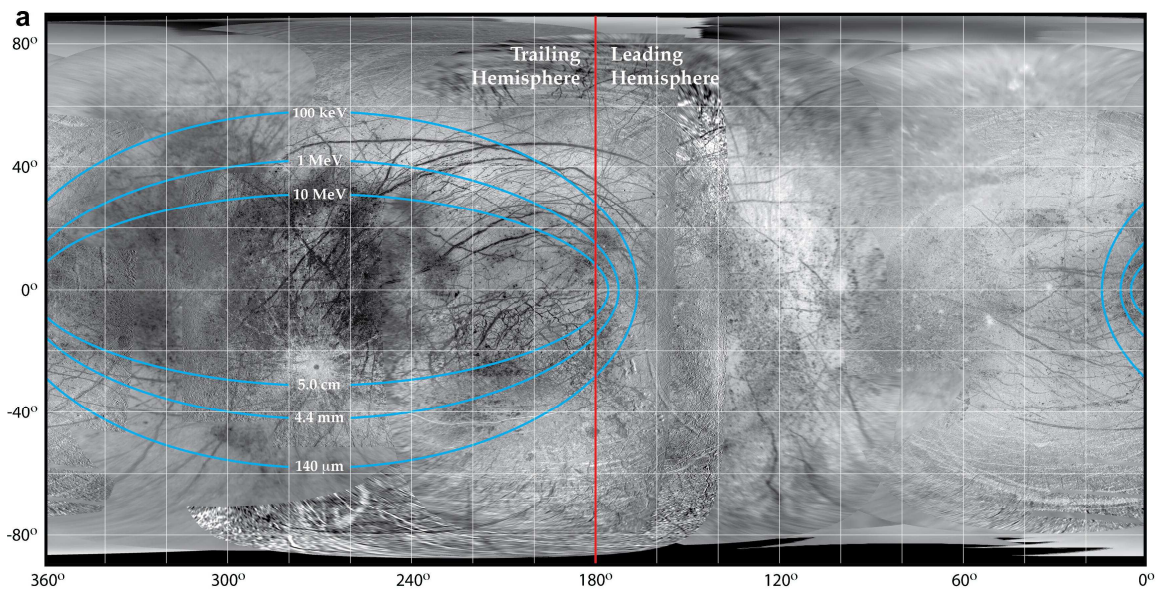


Figure13: Contour plot of electron bombardment of Europa where energies and penetration depths are indicated from Patterson et al. 2012)

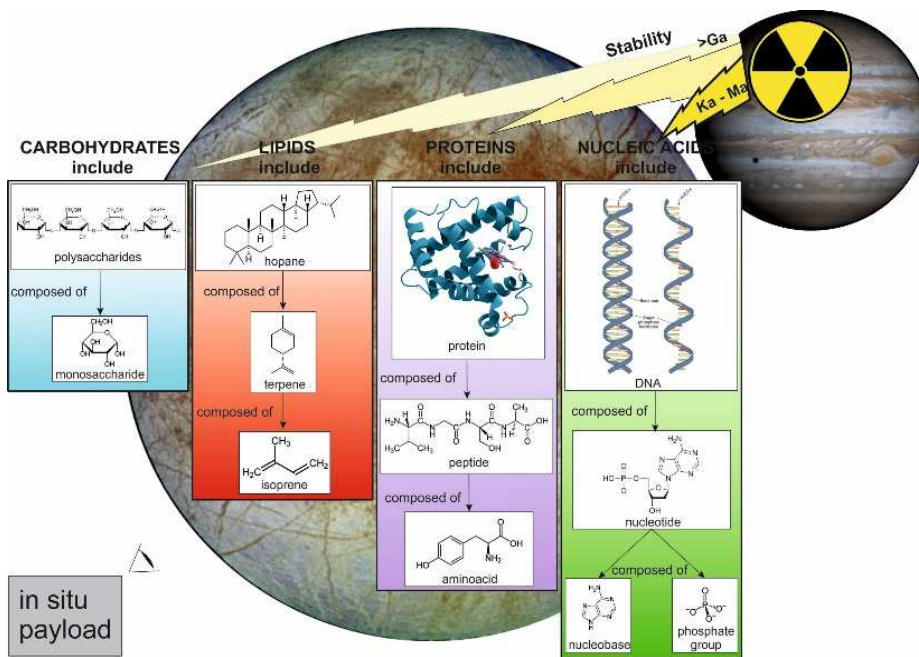


Figure 14: Types of biomolecules, from their monomers to the more complex polymers. Their higher stability under radiation is marked by the lower intensity of the yellow colour of the ray.

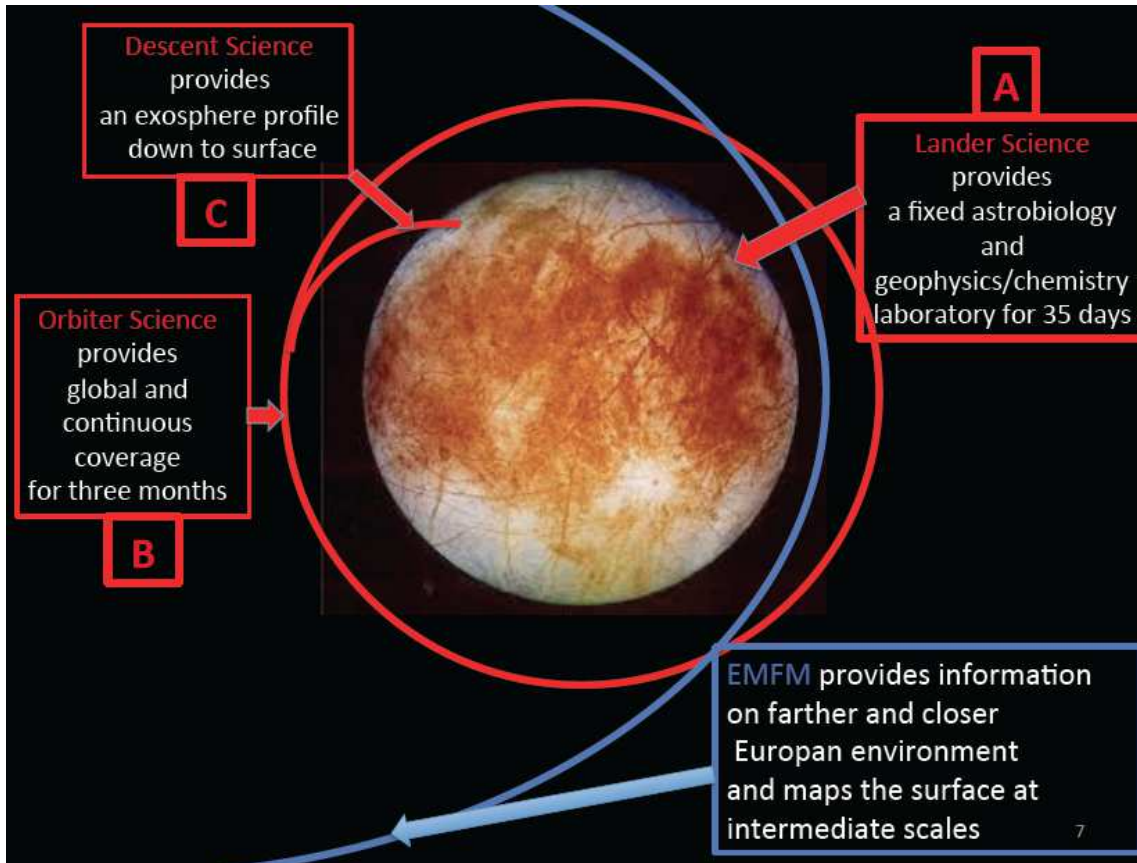


Figure 15: the JEM Observing system, with its two main platforms, will provide three main science sequence, complemented by VLBI astrometry measurements from Earth.

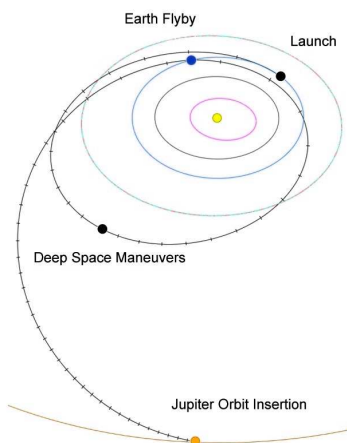


Figure 16: S1 - Interplanetary cruise

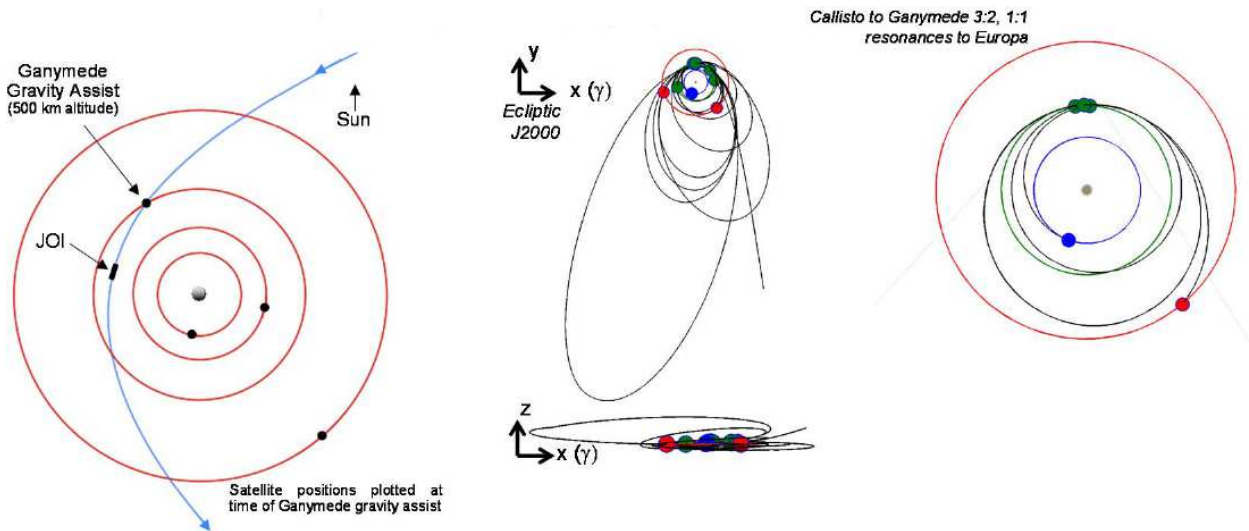


Figure 17: S2 - Jupiter orbit insertion (left) and figure) & S3 - Jovian tour. This tour starts with a series of eccentric orbits whose apojove and inclination are progressively reduced (center figures, projections in the YX (top) and XZ (bottom) planes, and continues with a set of low-eccentricity orbits in the equatorial plane to progressively approach Europa (blue spot), using its mean motion resonance with Callisto (red spot).

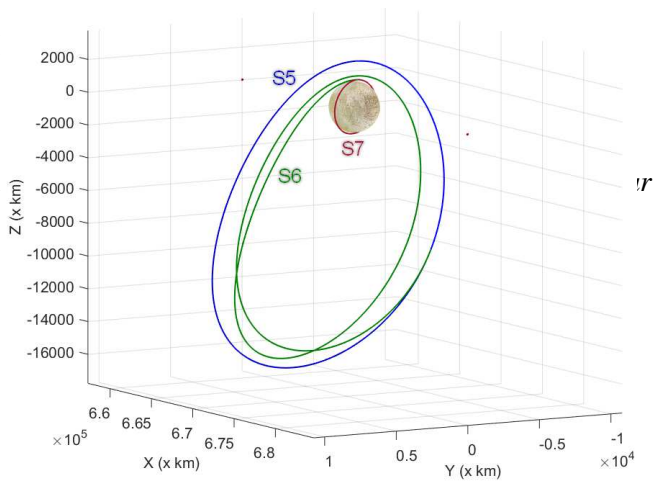


Figure 18: configuration of the Europa science orbits: halo orbit about the L1 Lagrangian point (blue, S5); transfer to Low Europa Orbit (green, S6) and finally low quasi-polar Europa orbit (red, S7).

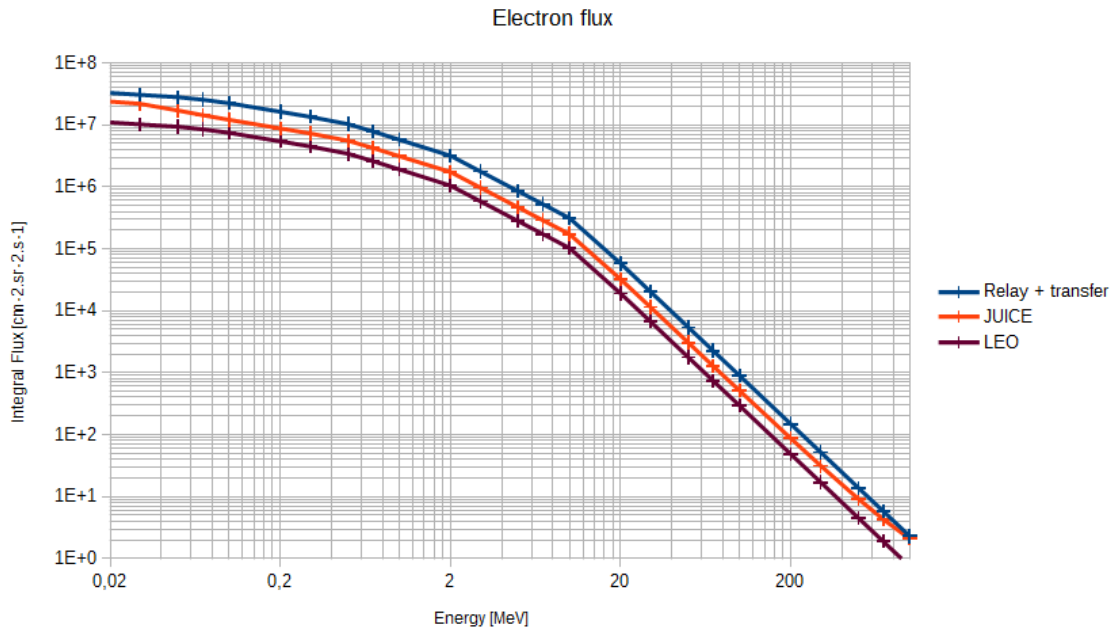


Figure 19: Integral electron flux vs. energy from SPENVIS, displayed for various phases of the JEM and compared to JUICE worst-case.

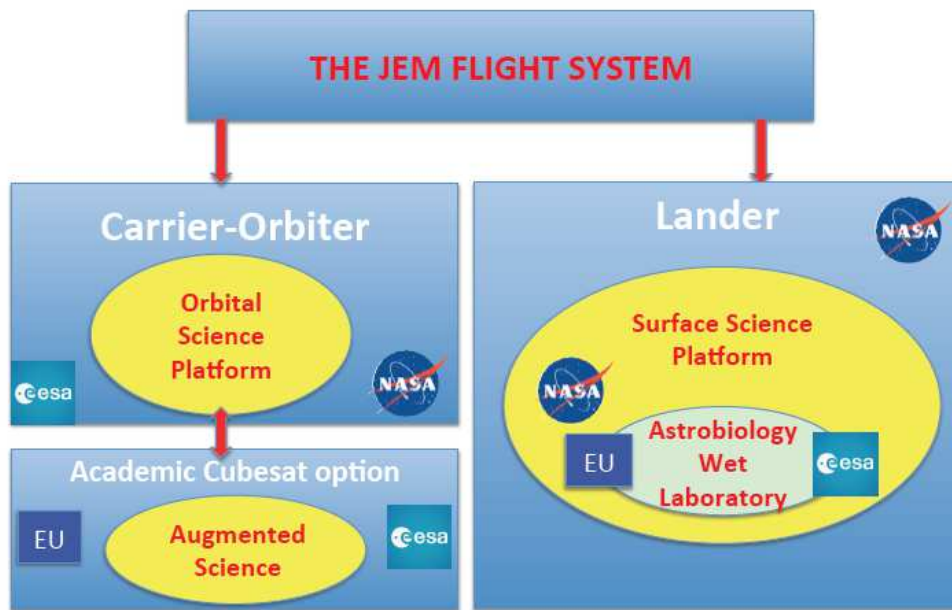


Figure 20: Overall architecture of the proposed JEM flight system, with its different flight elements.

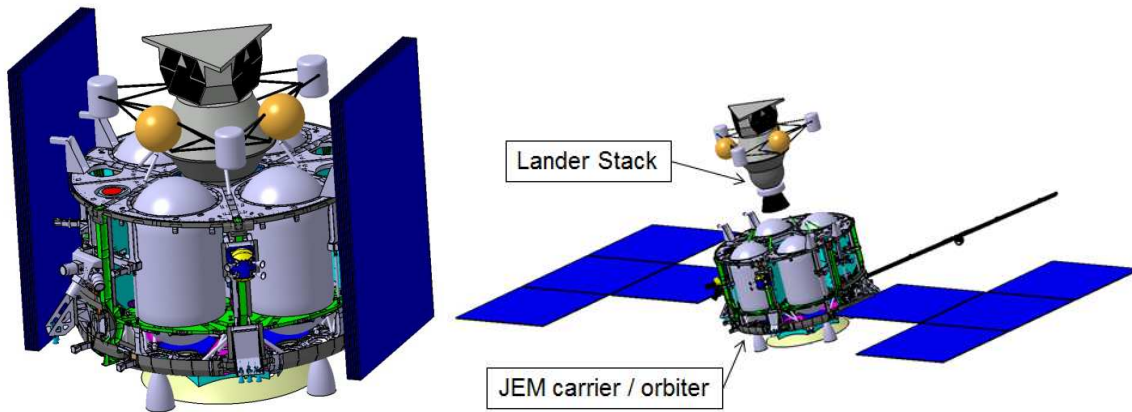


Figure 21: JEM carrier and lander interface

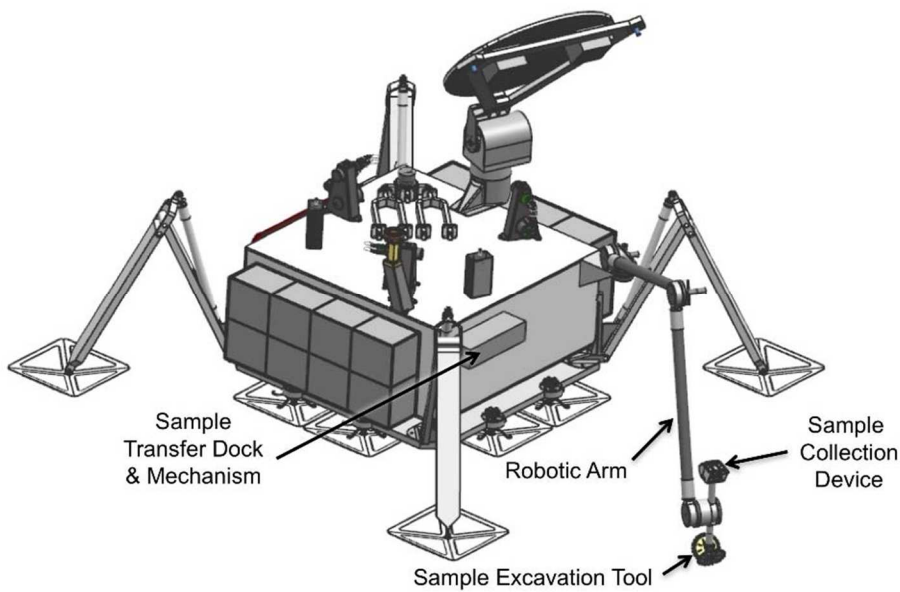


Figure 22: The NASA Europa lander concept presented in the Europa Lander Science Definition Team report (K. Hand et al., 2017).

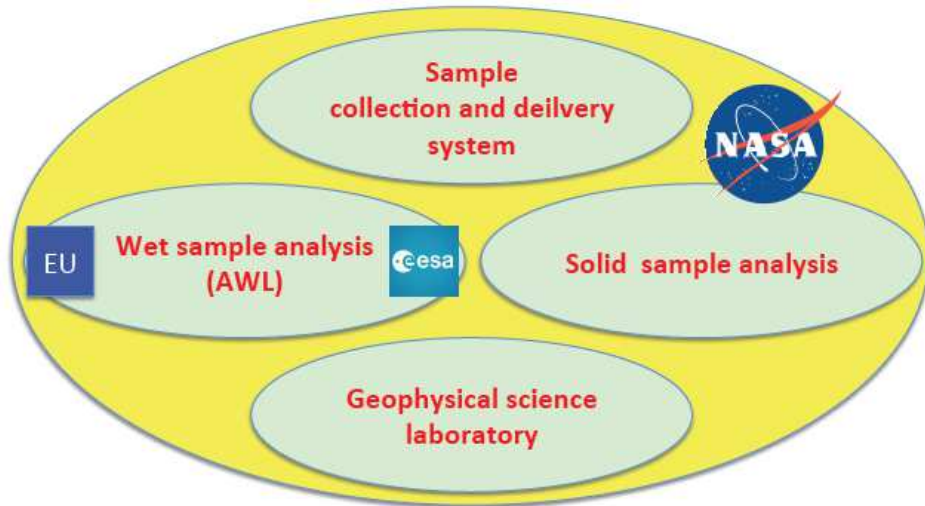


Figure 23: Proposed functional structure of the surface science platform on board the soft lander.

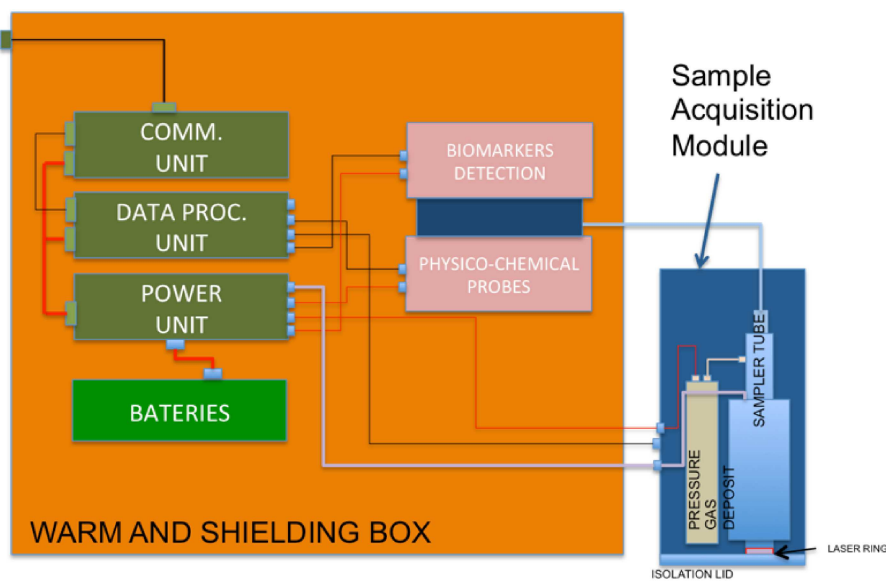
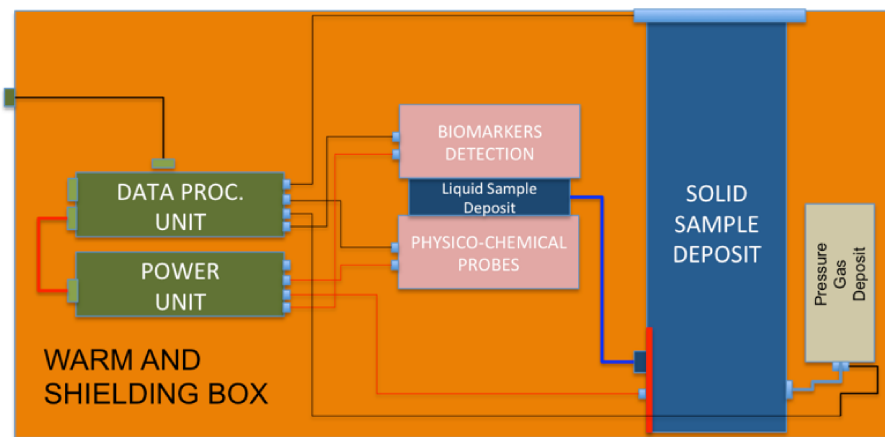
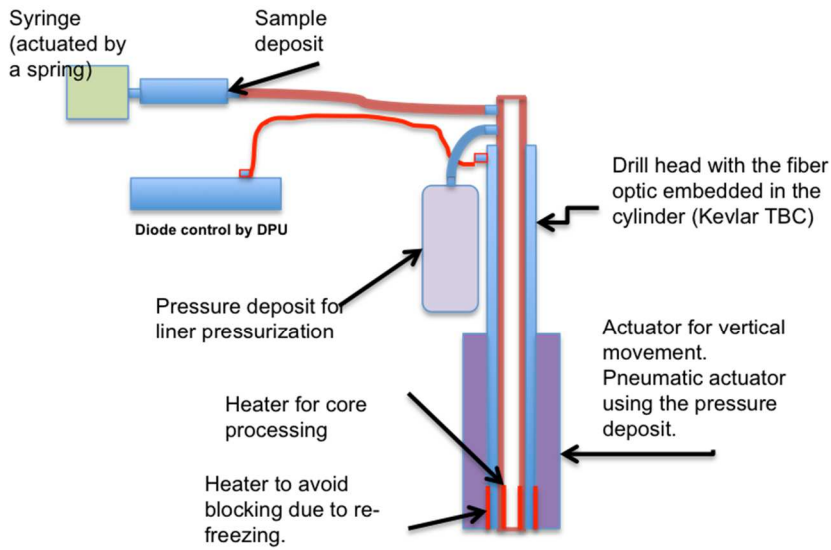


Figure 24: AWL/L (top) Block Diagram in case it is accommodated inside the lander and AWS/S in case it is deployed at the surface



Power estimated 10 watts for 1 hour of drilling TBC. (with pneumatic actuator).

Figure 25: Sample acquisition concept.

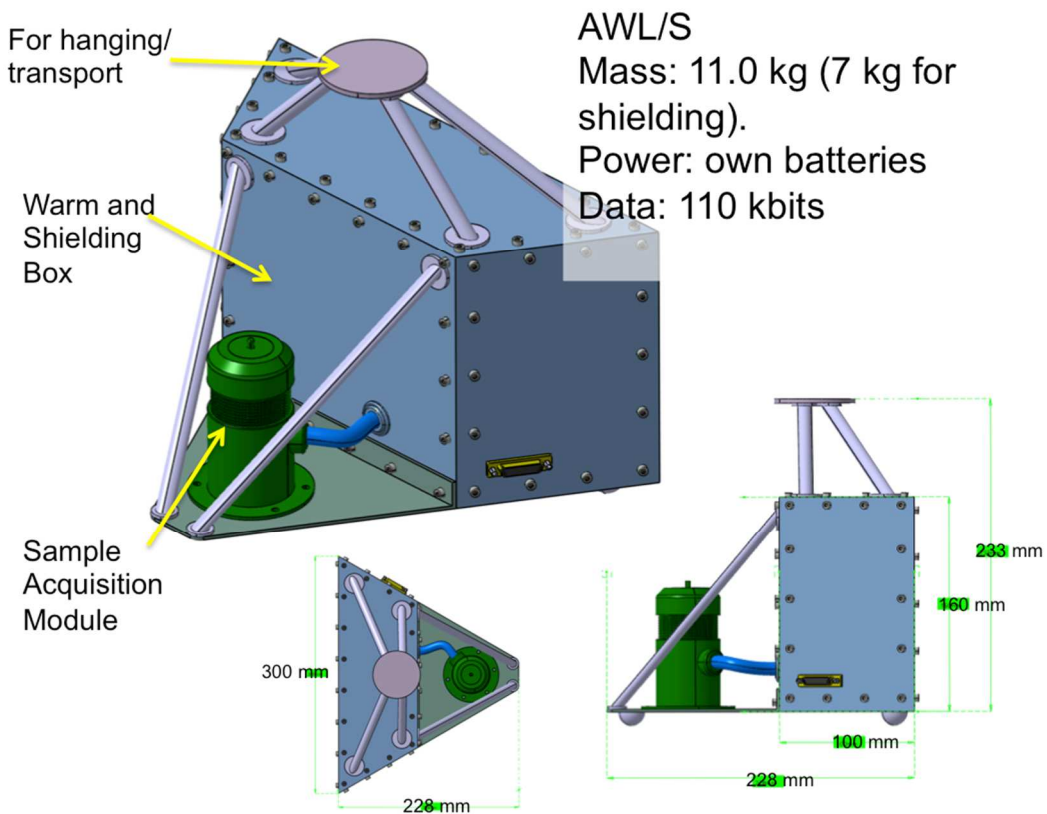


Figure 26: AWL/S mechanical configuration concept. A support structure allows it to be handled by the lander arm. A box protects the electronics, MAP and MPP. The isolation lid, below SAM, has a lateral movement to be open.

Annex II: JEM orbiter system design

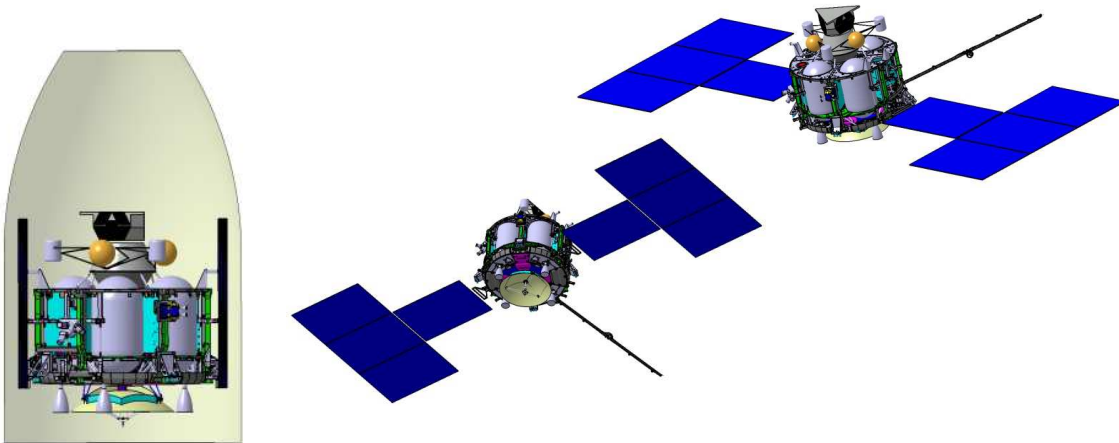


Figure A2.1: Spacecraft configuration (stacked and deployed)

ANNEX III: Orbitography for the JEM mission

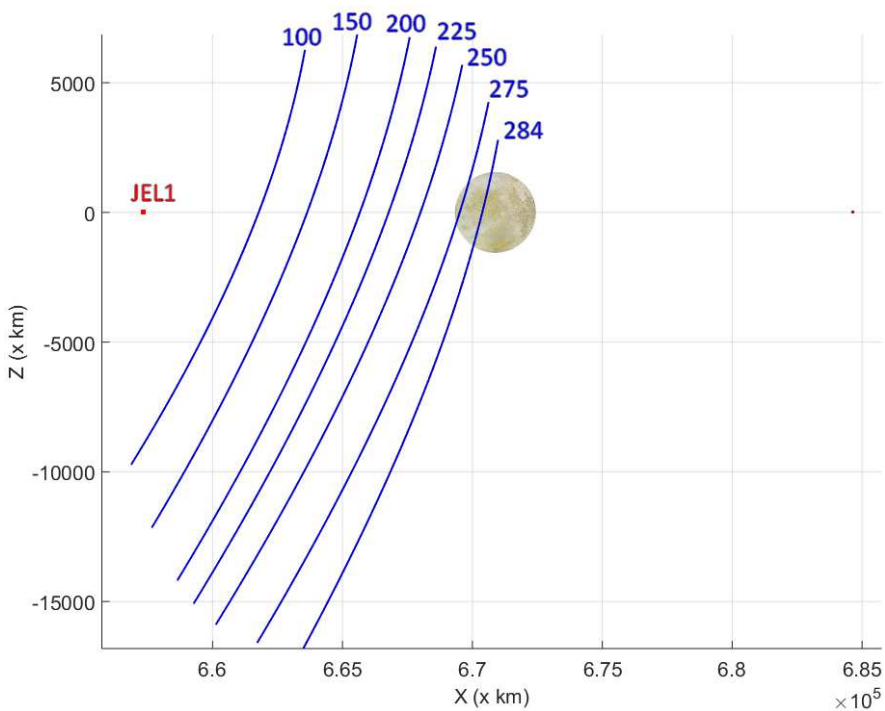


Figure A3.1: A set of JEL1 southern halo orbit in Jupiter-Europa rotating frame

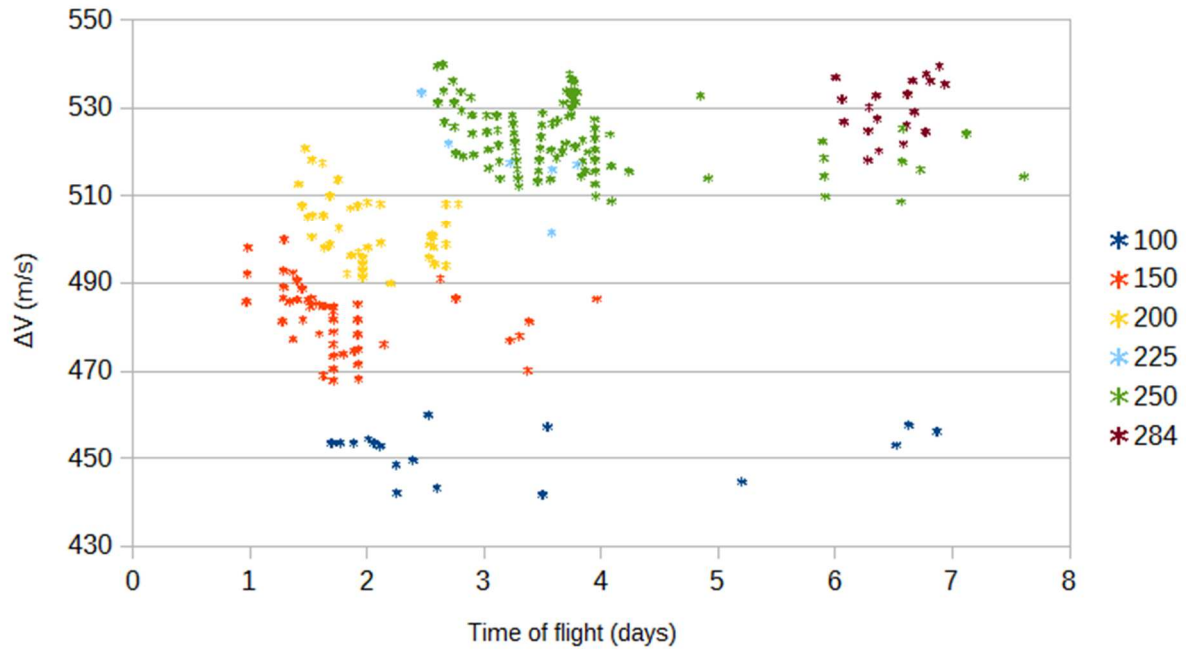


Figure A3.2: ΔV vs Time of flight for all the possible transfers of a set of halo orbits

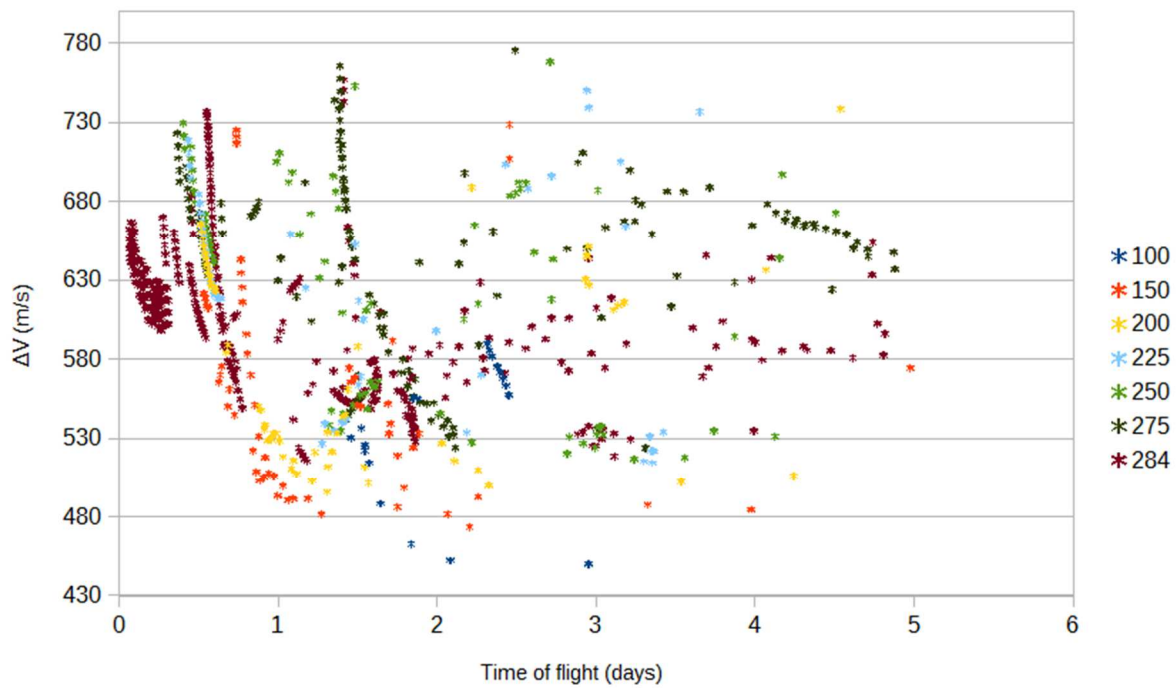


Figure A3.3: ΔV vs Time of flight for all the possible transfers with a tangent burn to leave a set of halo orbits

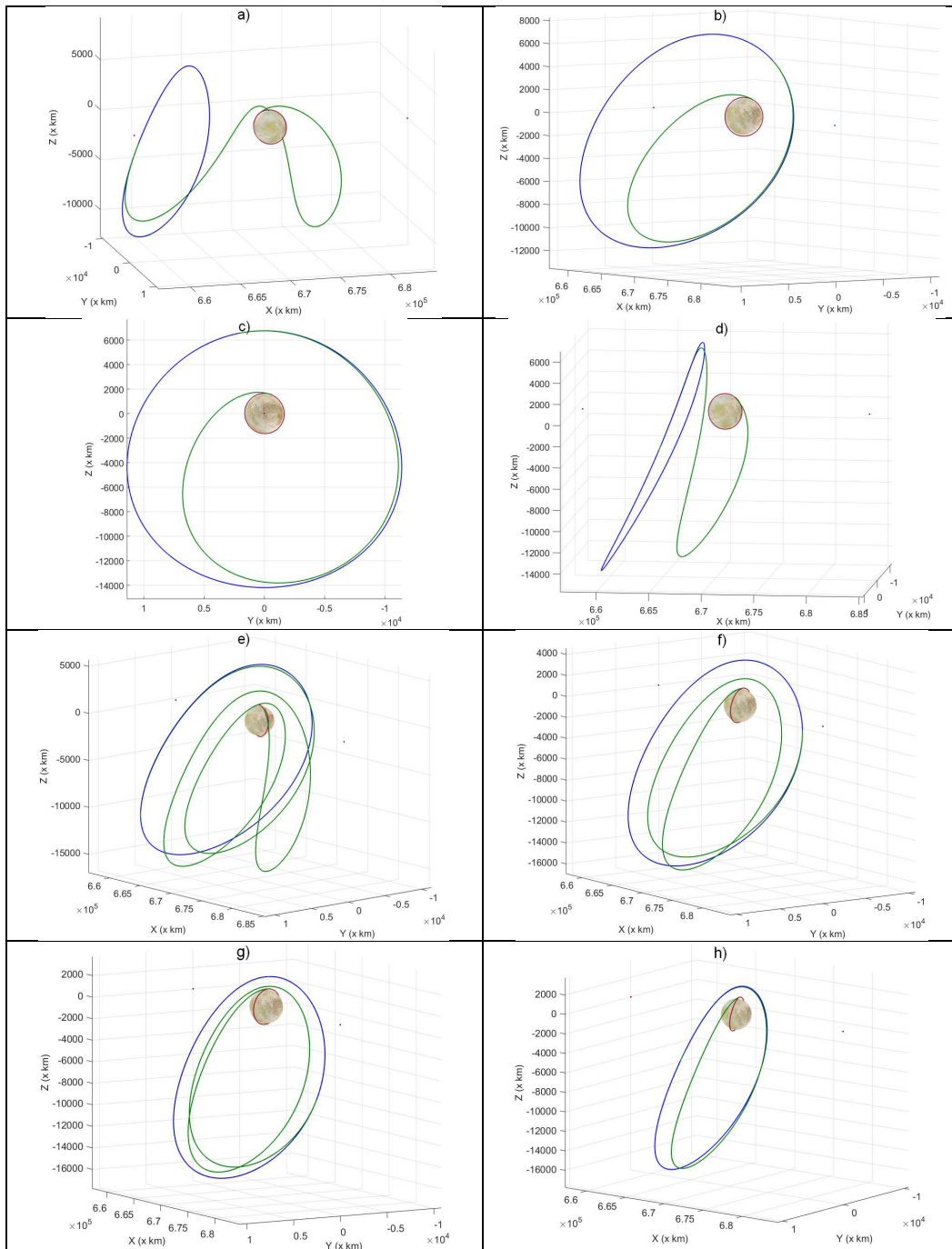


Figure A3.4: Set of transfers using different halo orbits

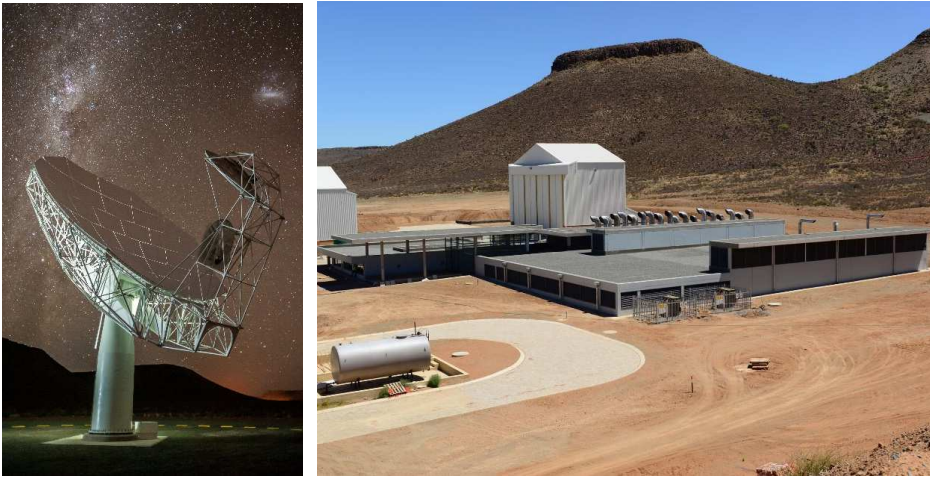


Figure A4.1: MeerKAT Dish (Left) and Karoo Array Processor Building (Right)

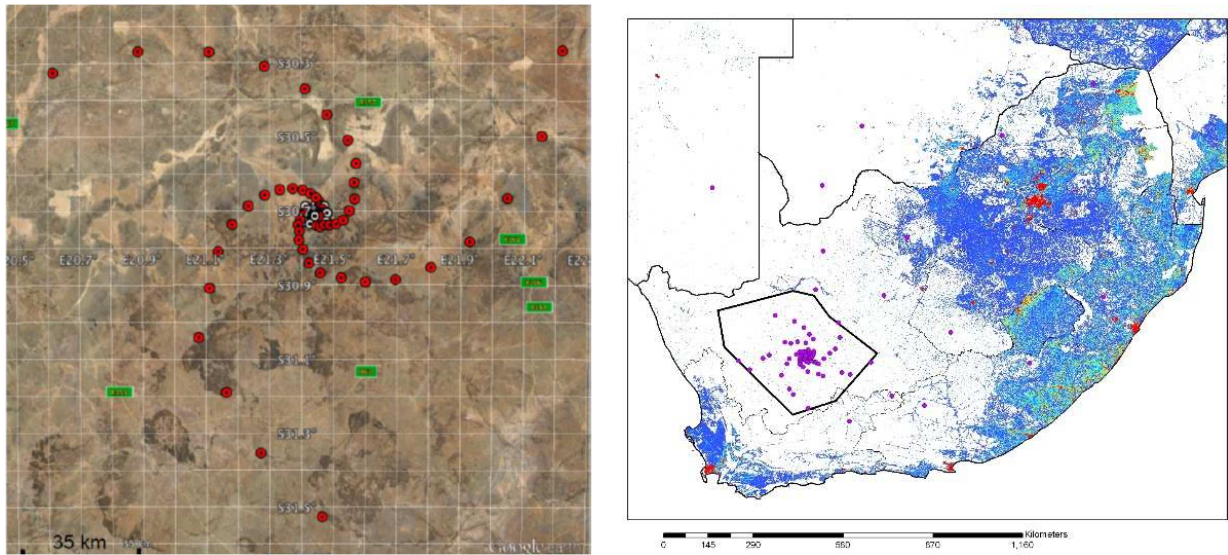


Figure A4.2: SKA1-Mid Array Configuration (Left) and SKA1-Mid Array Location in South Africa (Right, Showing Population Density and an Older Array Config)

Table 1: Proposed list of orbiter platform instruments and their contribution to the different Priority Science Objectives (PSO's) presented in section 2.

Orbiter Science Platform - JEM (Orbiter-Carrier) ESA/NASA		
	Facility/Instrument	Reference PSO
Core Payload	Gravity Science Investigation (GSI)	PSO#2, PSO#4
	Magnetometer (MAG)	PSO#1, PSO#3, PSO#4
	Laser Altimeter (LA)	PSO#2, PSO#4
	Ion Mass Spectrometer + Electron Spectrometer (IMS/ELS)	PSO#1, PSO#3, PSO#5
	Ion and Neutral Mass Spectrometer (INMS)	PSO#3, PSO#5
	Dust Analyser (DA)	PSO#1, PSO#3, PSO#5
Augmentation	Langmuir Probe (LP)	PSO#1, PSO#3

Table 2: Projected resource requirements for the different orbiter platform instruments.

Orbital Science Platform projected required resources						
Facility/Instrument	Outside the vault	Inside the vault				
		Mass (kg)	Volume (m ³)	Total (kg)	Power (W)	TRL
GSI	-	3.4	0.006	3.4	22	5
<u>MAG</u>	<u>0.1</u>	<u>0.1</u>	0.001	<u>0.2</u>	<u>0.4</u>	<u>8/9</u>
LA	11	9	0.08	20	40	5-6
IMS/ELS	7	3	0.006	10	11	5
<u>INMS</u>	3.2	3	0.006	6.2	16	5-6
<u>DA</u>	<u>7.5</u>	<u>2.6</u>	<u>0.003</u>	<u>10.1</u>	<u>9.7</u>	<u>5-6</u>
<u>Total for core payload</u>	28.8	21.1	0.102	49,9	99.1	
<u>Augmentation: LP</u>	<u>1.6</u>	<u>3</u>	<u>0.004</u>	4.6	<u>6</u>	5-6

Table 3: Proposed list of surface science platform instruments and their contribution to the different Priority Science Objectives (PSO's) presented in section 2.

Surface Science Platform - JEM (Lander) NASA	
Facility/Instrument	Reference PSO
1. Solid Sample Analysis	
Organic compound analyzer	PSO#4, PSO#5
Vibrational Spectrometer	
Microscope	
PanCam	
2. Liquid Sample Analysis Astrobiological Wet Laboratory	
Multiprobe Array Sensors (MPAS)	PSO#5
Multiparametric Probes (MPP)	PSO#5
3. Geophysical Science	
Geophone	PSO#2, PSO#4
Magnetometer	PSO#1
Laser reflector	PSO#2

Table 4: Projected resource requirements for the different instruments of the surface science platform.

Surface Science Platform projected required resources			
Facility/Instrument	Mass (kg)	Power (W)	TRL
AWL sensors MPAS	0.15	1.4	3-4
AWL sensors MPP	0.1	1	3-4
AWL sensors VISTA		0.24	5-6
Total for AWL (cf. 4.3.3.2)	11 (incl. 7 for shielding)	17.4 Whr	
MAG	0.6	0.8	8/9
Laser Reflector	0.0025	-	-

Table 5: approximate flight time ΔV and TID (behind 2,5 mm finite Al slab shell)

Sequence	Sequence name		Flight time	ΔV (m/s)	TID @ 2.5mm Al
S-1	Launch + cruise	Reach Jupiter System	4,9 years	800	~
S-2	JOI + PRM maneuver	Insert into the Jovian system	6,5 months	1000	~
S-3	Jovian tour to Europa vicinity	Phase the spacecraft with Europa	9,5 months	100	125 krad
S-4	EOI +	Insert into Europa,		700	~

	Ejection to relay orbit	release the lander, reach relay orbit			
S-5	Lander relay	Relay and downlink lander data	35 days	~	370 krad
S-6	Relay to LEO	Reach low-altitude quasi-polar orbit	1-3 days	400 (TBC)	12 krad/day
S-7	LEO operations	Support orbiter science mission	3 months	50	930 krad
S-8	Descent to surface				
S-9	Impact	End of mission			
<u>Total</u>			6,6 years	<u>3,05 km/s</u>	1,5 Mrad

Table 6: Total Ionizing Dose (TID, in krad) versus Aluminium thickness (in mm) for the relay phase, the transfer to Low-Europa Orbit (LEO), the science orbit as well as the total for these three phases. For the relay and transfer phases, the second column corresponds to the worst case scenario with a radiation design factor of 2; for the LEO the second column corresponds to the case where the reduced radiation environment at low-altitude around Europa is taken into account (factor 3 reduction), and the third column to the worst case scenario with a radiation design factor of 2. The values obtained are very similar to those reported in the 2012 NASA Europa Orbiter report.

Al absorber thickness (mm)	S5 - Lander relay TID (krad)		S6 - Relay to LEO TID (krad)		S7 - LEO operations TID (krad)			S5 to S7 - Total TID (krad)		
	<i>no margin</i>	<i>margin x2</i>	<i>no margin</i>	<i>margin x2</i>	<i>no margin</i>	<i>Europa shield.</i>	<i>margin x2</i>	<i>no margin</i>	<i>Shield/no marg</i>	<i>margin x2</i>
2,5	369	738	12,3	24,6	930	310	620	1311	691	1382
3	299	598	9,98	20,0	753	251	502	1062	560	1120
4	207	414	6,91	13,8	521	174	347	735	388	775
5	152	304	5,07	10,1	382	127	254	539	284	568
6	117	233	3,89	7,77	293	97,6	195	413	218	436
7	92,61	185	3,09	6,18	233	77,5	155	328	173	346
8	75,6	151	2,52	5,04	190	63,2	126	268	141	283
9	62,9	126	2,10	4,19	158	52,6	105	223	118	235
10	53,2	106	1,77	3,54	133	44,5	88,9	188	99,4	199
11	45,5	91,0	1,52	3,03	114	38,0	76,1	161	85,1	170
12	39,3	78,6	1,31	2,62	98,6	32,9	65,8	139	73,5	147
13	34,2	68,5	1,14	2,28	85,9	28,6	57,2	121	64,0	128
14	30,0	60,0	1,00	2,00	75,3	25,1	50,2	106	56,1	112
15	26,5	53,0	0,88	1,76	66,4	22,1	44,3	93,8	49,5	99,0
16	23,5	46,9	0,78	1,56	58,8	19,6	39,2	83,1	43,9	87,7
17	20,9	41,8	0,70	1,39	52,4	17,5	34,9	74,0	39,1	78,1
18	18,7	37,4	0,62	1,24	46,8	15,6	31,2	66,1	34,9	69,8
19	16,7	33,5	0,56	1,12	42,0	14,0	28,0	59,3	31,3	62,6
20	15,1	30,1	0,50	1,00	37,7	12,6	25,2	53,3	28,1	56,3

22	12,3	24,6	0,41	0,82	30,8	10,3	20,5	43,5	23,0	45,9
25	9,23	18,5	0,31	0,61	23,1	7,70	15,4	32,6	17,2	34,5

Table 7: summarized characteristics of the Sample Analysis Module (SAM)

MAIN TECHNICAL CHARACTERISTICS OF SAM
Drilling activities consumption 10 W for 1 hour.
Additional sample processing 2.5 W for 3 hour.
Data processing & control core consumptions 5W.
Orbiter has the capacity to charge and monitor the battery (req. 85 W.hr)
Battery should be maintained warmed to $T > -20^{\circ}\text{C}$
No redundancy
Standard flight EEE components
Control based on a FPGA running a low frequency
S/W in coded C and small program size < 64 KB
Power conditioning based on COTS converter
Orbiter has the capacity to charge and monitor the battery (req. 145 W.hr including AWL self heating).
Battery configuration 5 series-cell & 5 parallel cells. Total weight < 1.5 kg.

Table A2.1: JEM projected mass budget and ISP.

Carrier dry mass	2 485 kg	
Lander Stack mass	2 800 kg	
ISP	315 s	R-4D 490 N

Table A2.2: JEM deltaV and propellant budget

	Delta V (m/s)	Propellant (kg)	Wet mass (kg)	Comment
Cruise (DSM / EGA)	800	3 002	13 163	4,9 years transfer (DVEGA)
JOI + PRM	1 000	2 809	10 160	840 JOI + 160 PRM
Jupiter Tour	100	234	7 351	Europa 2012 study
EOI	600	1 256	7 117	elliptical orbit 200×7000 km
Ejection to relay	100	187	5 861	allocation
Relay to science	400	349	2 875	200×200 km
Orbit maintenance	50	41	2 526	3 months in orbit
Total	3 050	7 878	13 163	

Table A3.1: Characteristics of the range of the reachable LEO

ID	Inclination (°)		Altitude (km)	
	min	max	min	max
100	82,8	89,8	116	198
150	83,4	89,8	103	200
200	80,2	82,9	104	199
225	88,1	89,7	109	196
250	80,5	87,8	101	199
275	-	-	-	-
284	81,1	88,7	102	185

Table A3.2: Characteristics of some of the reachable LEO

ID	Inclination (°)		Altitude (km)	
	min	max	min	max
100	80,0	89,9	100	190
150	80,2	90,0	102	199
200	80,1	90,0	103	199
225	80,1	89,9	102	199
250	80,0	90,0	101	200
275	80,0	89,9	100	200
284	80,0	90,0	100	200

Table A3.3: Characteristics associated to the set of transfers

	Halo orbit ID	$\Delta V_{\text{total}}(\text{m/s})$	Duration (days)	Altitude (km)	Inclination (°)
a)	100	488	1,6	118	84,8
b)	150	491	1,2	110	85,5
c)	200	512	1,3	104	82,6
d)	225	539	1,3	108	84,0
e)	250	534	3,7	104	87,6
f)	275	541	2,1	115	82,4
g)	284	551	1,8	119	84,3
h)	284	515	1,2	199	80,8